MOLECULAR AND CELLULAR BIOLOGY, Sept. 2008, p. 5403–5419 Vol. 28, No. 17
0270-7306/08/$08.00+0 doi:10.1128/MCB.00739-08

hnRNP H and hnRNP F Complex with Fox2 To Silence Fibroblast Growth Factor Receptor 2 Exon IIIc▽†

David M. Mauger,[1,2] Carolina Lin,[3] and Mariano A. Garcia-Blanco[1,2,4]*

Department of Molecular Genetics and Microbiology,[1] Center for RNA Biology,[2] Program in Cell and Molecular Biology,[3] and Department of Medicine,[4] Duke University Medical Center, Durham, North Carolina 27710

Received 8 May 2008/Accepted 10 June 2008

The heterogeneous nuclear ribonucleoprotein H (hnRNP) family of proteins has been shown to activate exon inclusion by binding intronic G triplets. Much less is known, however, about how hnRNP H and hnRNP F silence exons. In this study, we identify hnRNP H and hnRNP F proteins as being novel silencers of fibroblast growth factor receptor 2 exon IIIc. In cells that normally include this exon, we show that the overexpression of either hnRNP H1 or hnRNP F resulted in the dramatic silencing of exon IIIc. In cells that normally skip exon IIIc, skipping was disrupted when RNA interference was used to knock down both hnRNP H and hnRNP F. We show that an exonic GGG motif overlapped a critical exonic splicing enhancer, which was predicted to bind the SR protein ASF/SF2. Furthermore, the expression of ASF/SF2 reversed the silencing of exon IIIc caused by the expression of hnRNP H1. We show that hnRNP H and hnRNP F proteins are present in a complex with Fox2 and that the presence of Fox allows hnRNP H1 to better compete with ASF/SF2 for binding to exon IIIc. These results establish hnRNP H and hnRNP F as being repressors of exon inclusion and suggest that Fox proteins enhance their ability to antagonize ASF/SF2.

The heterogeneous nuclear ribonucleoproteins (hnRNPs) are a large group of nuclear RNA binding proteins, several of which regulate mRNA splicing. The protein family of hnRNP H and hnRNP F is one group of hnRNPs that have been found to play important roles in the regulation of alternative splicing decisions (5). hnRNP H and hnRNP F are two closely related proteins that bind to the RNA sequence DGGGD (6). Intriguingly, hnRNP H has been shown to have either enhancing or silencing activity, depending on the context of the binding site. On the one hand, hnRNP H activates exon inclusion by binding G-rich intronic elements downstream of the 5′ splice site in c-*src* (15, 29), human immunodeficiency virus type 1 (HIV-1) (7), Bcl-X (22, 34), GRIN1 (23), and myelin (34) transcripts, while on the other hand, it silences exons when bound to exonic elements in β-tropomyosin (14, 21), HIV-1 (20, 24), and α-tropomyosin (16) transcripts. Recently, Martinez-Contreras et al. proposed that the hnRNP H/F family, as well as the hnRNP A/B family, could stimulate the splicing of long introns in vitro by binding near the ends of these introns and dimerizing, thus looping out the intron (26). The fact that the function of hnRNP H and hnRNP F depends upon context suggests that the poorly understood mechanism by which hnRNP H and hnRNP F regulate exons involves a complex series of RNA-protein and protein-protein interactions.

Although the mechanism of splicing regulation is poorly understood, the domains of the hnRNP H and hnRNP F proteins have been well characterized. Figure 1 shows an alignment of the amino acid sequences for hnRNP H and hnRNP F family members: hnRNP H1 (GenBank accession number NP_005511), hnRNP H2 (accession number NP_001027565), hnRNP F (accession number NP_001091674), and the two alternatively spliced isoforms of hnRNP H3 (accession numbers NP_036339 and NP_067676.2). hnRNP H1 and hnRNP H2 are 96% identical at the amino acid level and 87% identical at the nucleotide level. hnRNP F is 68% identical to hnRNP H1 at the amino acid level, and the conservation through the third RNA recognition motif (RRM) is ~80% identity. hnRNP H3 is a smaller protein that is the most divergent family member, with 48% identity to hnRNP H1; however, H3 is 71% identical to H1 in the region spanning the last two RRMs. The alignment in Fig. 1 shows a high level of conservation among all H and F family members within the three annotated RRMs, except for RRM1, which is absent in hnRNP H3. Dominguez and Allain previously demonstrated that both RRM1 and RRM2 can bind to the RNA at DGGGD motifs, while RRM3 did not (19). They solved the structure of each of the RRMs in hnRNP F using nuclear magnetic resonance spectroscopy, and their analysis indicated that the conserved residues W20 and Y82 in RRM1 and F120 and Y180 in RRM2 directly contact the RNA (19). In addition to these RRMs, H and F proteins have an extensive glycine-rich region near the carboxy terminus, which is highlighted in Fig. 1 by the circling of the glycine residues near the carboxy terminus. This domain may allow members of the H/F family to homo- or heterodimerize. hnRNP H and hnRNP F have been shown to coimmunoprecipitate (15), and a similar glycine-rich domain in hnRNP A1 was previously shown to be both necessary and sufficient to induce the silencing of an exon when artificially recruited to it (17, 27).

hnRNP A1 is a related protein that has been characterized as a splicing silencer, often acting in opposition to an activating hnRNP H. Studies of the c-*src*, HIV, GRIN1, and β-tropomyosin transcripts have shown that exons within these alterna-

* Corresponding author. Mailing address: Box 3053 (424 CARL), Duke University Medical Center, Research Drive, Durham, NC 27710. Phone: (919) 613-8632. Fax: (919) 613-8646. E-mail: garci001@mc.duke.edu.

† Supplemental material for this article may be found at http://mcb.asm.org/.

▽ Published ahead of print on 23 June 2008.

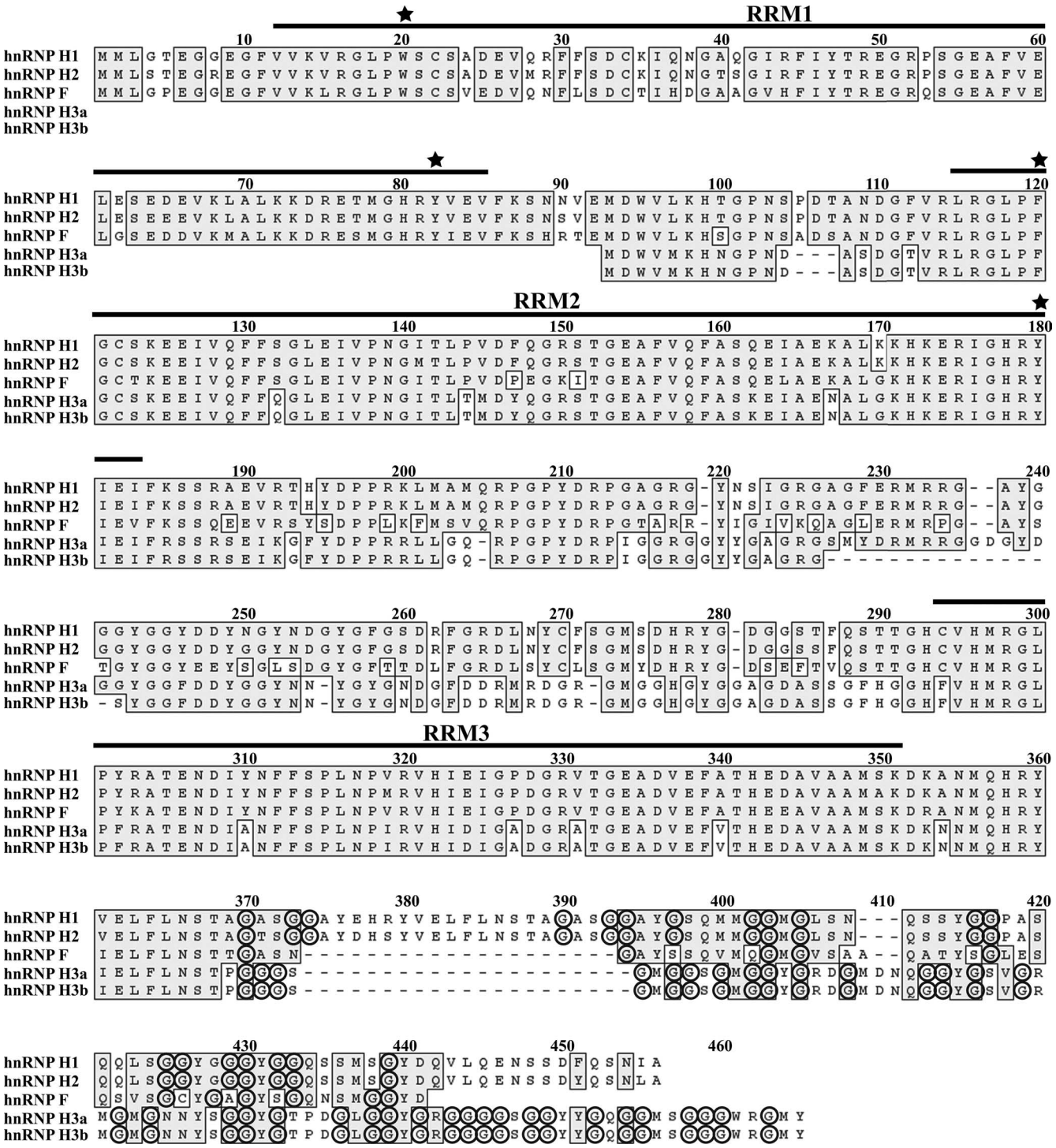

FIG. 1. Amino acid conservation of the hnRNP H/F family. Shown is an alignment of the amino acid sequences for hnRNP H1, hnRNP H2, hnRNP F, and hnRNP H3. The alignment displays both isoforms of the hnRNP H3 transcript (hnRNP H3a and hnRNP H3b), which arise from an alternative splicing event. Residues are blocked if they are identical or synonymous in the majority of the family members, and the annotated RRMs are indicated by a labeled black bar located above the sequence. Amino acids W20, Y82, F120, and Y180 are marked above the sequence with stars. These residues are conserved throughout the family and have been demonstrated to directly contact the RNA. Glycine residues in the glycine-rich region near the carboxy terminus are highlighted by circles around the residues.

tively spliced transcripts are silenced by hnRNP A1 (2, 21, 23, 30, 39). The overall domain structure of the hnRNP A/B family is reminiscent of that of the hnRNP H/F family. The A and B proteins have two RRMs, followed by a long glycine-rich region at the carboxy terminus. Other researchers found that the mutation of either the RRMs or the glycine-rich region of hnRNP A1 disrupted the ability of this protein to silence exons in vitro and that the deletion of the glycine-rich domain also

disrupted the ability of the remaining RRMs to bind efficiently to RNA (1, 27, 28). The importance of protein-protein interactions to the function of hnRNP A1 led to the creation of the nucleated binding model of exon silencing. This model proposed that high-affinity sites of binding to hnRNP A1 could nucleate the binding of hnRNP A1 molecules to remote lower-affinity binding sites and that this recruitment allowed hnRNP A1 to displace several critical splicing factors such as SR proteins (40). The importance of the competition of hnRNP A1 with SR proteins for binding to the RNA was further established by studies of the c-*src* and GRIN1 transcripts, where hnRNP A1 binding sites were found near, but not overlapping, binding sites for SR proteins (23, 30). Nonetheless, in both of these cases, the evidence supported the nucleated binding model, as mutations that disrupted both the hnRNP A1 site as well as the SR protein site resulted in a disruption of exon silencing. This suggested that hnRNP A1 did more than simply block the recruitment of an SR protein at that specific site (23, 30). Additionally, the glycine-rich domain induces silencing when artificially recruited to an exon through an MS2-coat protein fusion (17). Combined, these studies highlight the central role that protein-protein interactions play in the mechanism by which the hnRNP A/B family silences exons. Whether or not a similar mechanism applied to the structurally similar hnRNP H/F family remained to be determined.

In this study, we establish hnRNP H and hnRNP F as being regulators of the alternative splicing of the fibroblast growth factor receptor 2 (FGFR2) transcripts. The FGFR2 transcript undergoes a mutually exclusive alternative splicing event where the mature mRNA contains either exon 8, also known as exon IIIb, or exon 9, also known as exon IIIc (8, 9, 13). We previously showed that the Fox family of splicing regulators silenced exon IIIc by binding to UGCAUG elements upstream and within exon IIIc (4). Immediately upstream of the exonic UG CAUG element, we noticed three GGG motifs, and this led us to ask if hnRNP H and hnRNP F played a role in silencing the exon. Here, we show that the overexpression of hnRNP H or hnRNP F can efficiently silence exon IIIc in cells where that exon is normally included. We demonstrate by RNA interference (RNAi) knockdown that either hnRNP H or hnRNP F was required for the efficient silencing of exon IIIc. Similar to results for hnRNP A1, a structure-function analysis revealed that this silencing activity was dependent on the first two RRMs. Surprisingly, in stark contrast with hnRNP A1, the carboxy-terminal 160 amino acids, including the third highly conserved RRM and a glycine-rich region, were completely dispensable for silencing activity. hnRNP H and hnRNP F regulated the inclusion of exon IIIc through an interaction with the exonic GGG motifs, which functioned as exonic splicing silencers (ESSs). One of the motifs overlapped with an exonic splicing enhancer (ESE) that was predicted to bind the SR protein ASF/SF2, and the co-overexpression of ASF/SF2 fully rescued the inclusion of exon IIIc from hnRNP H1-induced silencing. We demonstrate that hnRNP H1 and ASF/SF2 compete with each other for cross-linking to labeled exon IIIc RNA. Additionally, we demonstrate that hnRNP H and hnRNP F are present in a complex with the tissue-specific splicing factor Fox2 and that the presence of Fox2 can affect the binding competition between hnRNP H1 and ASF/SF2. These findings establish hnRNP H and hnRNP F as being regulators of exon IIIc inclusion and imply that these proteins can cooperate with Fox proteins to block the recruitment of SR proteins to binding sites within the exon.

MATERIALS AND METHODS

Plasmid constructs. Minigene constructs pI12-DE-Fs, pI12-IIIc, pI12-IIIbS.S.Mut, pI12-IIIcS.S.Mut, pTracer-Fox-WT-V5-NLS, pTracer-Fox-Δ2-102-V5-NLS, pTracer-Fox-Δ294-377-V5-NLS, and pTracer-Fox-Δ206-377-V5-NLS were previously described (4, 10). The cloning of expression constructs (p3F-H1-WT, p3F-F, p3F-H3, p3F-ASF/SF2, p3F-H1-α, p3F-H1β, p3F-H1-Δ, p3F-H1-γ, p3F-H1-R1AA, p3F-H1-R2AA, p3F-H1-MutC1, p3F-H1-MutC2, and p3F-H1-MutC3), the mutagenesis of minigenes (pI12-3C-Mut1, pI12-3C-Mut2, pI12-3C-Mut4, pI12-3C-Mut4, pI12-3C-Mut6, and pI12-3C-Mut7), and in vitro transcription vector pT73C are described in Table S3 in the supplemental material. Inserts were amplified by PCR with the indicated oligonucleotides from the indicated templates and then cloned into the indicated vectors using the stated restriction enzymes and standard cloning techniques.

Cell culture and plasmid transfections. HEK293T and DT cells were cultured in low-glucose Dulbecco's modified Eagle's medium (Gibco) supplemented with 10% heat-inactivated fetal bovine serum (HyClone). Fusion proteins were overexpressed in cells as follows. One hundred thousand HEK293T cells were seeded into each well of a 12-well plate in 1.0 ml of medium without antibiotics. The cells were transfected 24 h later. Eight hundred nanograms of expression plasmids and 100 ng of minigene reporters were diluted to 100 μl with OptiMEM and then mixed with 5 μl of Lipofectamine 2000 (Invitrogen) diluted to 100 μl with OptiMEM. After 20 min of incubation, the reagent was gently added to the cells. Cells were grown for 48 h and harvested for RNA using TRIzol (Invitrogen) and for protein by sodium dodecyl sulfate (SDS) lysis as described below.

siRNA duplexes and knockdown of hnRNP H and hnRNP F. Four small interfering RNA (siRNA) duplexes that targeted rat hnRNP H (Dharmacon On-Target Plus) were ordered. The duplexes targeted the following sequences within the hnRNP H mRNA: H1 (5′-CAGUCGAGCUGAAGUUAGA-3′), H2 (5′-GAAGCAUACUGGUCCCAAU-3′), H3 (5′-GAGAGUACAUAUUGAG ACU-3′), and H4 (5′-UAACAUUGCCGGUGGACUU-3′). Three siRNA duplexes targeting rat hnRNP F were ordered (Qiagen HP GenomeWide siRNA). The duplexes targeted the following sequences: F1 (5′-AACGGAGAACGACA UUUACAA-3′), F2 (5′-AUGGGUGGAUAUGAUUAGUAU-3′), and F3 (5′-CCCGUUUGGAUGCACAAAGGA-3′). All duplexes were resuspended to a concentration of 20 μM, and pools of duplexes were created by mixing equal volumes of the 20 μM stocks. Knockdown experiments were done as follows. DT cells were seeded at 40,000 cells/well of a 24-well dish in 0.5 ml of medium without antibiotics. After 24 h, cells were transfected with individual siRNA duplexes or pools of duplexes to a final concentration of 20 nM as follows. For each well, 0.6 μl of 20 μM siRNA duplex was diluted to 50 μl with OptiMEM and mixed with 0.6 μl of Lipofectamine 2000 (Invitrogen) diluted to 50 μl with OptiMEM. The mixture was incubated for 20 min at room temperature and then gently added to the cells. Twenty-four hours after transfection, the cells were washed in phosphate-buffered saline (PBS), trypsinized with 200 μl of trypsin-EDTA, and resuspended in growth medium. The cells were counted, and 80,000 cells were seeded into each well of a 12-well dish in 1.0 ml of medium. Twenty-four hours after reseeding, the cells were transfected with a minigene reporter and a second dose of the same siRNA duplex. For each well, 0.6 μl of 20 μM siRNA duplex and 50 ng of minigene reporter were mixed and diluted to 100 μl with OptiMEM. This solution was added to 0.725 μl of Lipofectamine 2000 (Invitrogen) diluted to 100 μl with OptiMEM, and the mixture was incubated for 20 min at room temperature. Two hundred microliters of this reagent was added to cells. Cells were grown for 48 h, and RNA was harvested using TRIzol (Invitrogen) and for protein by SDS lysis.

RNA isolation and RT-PCR assay for transfected minigenes. Splicing products of minigenes were analyzed by semiquantitative reverse transcription-PCR (RT-PCR) analysis as previously described (10). Products were amplified with primers specific to the upstream (T7 [5′-GTAATACGACTCACTATAGG-3′]) and downstream (SP6 [5′-GATTTAGGTGACACTATAG-3′]) adenovirus exons. Splicing products containing only exon IIIb or exon IIIc were distinguished by analytical digestion with AvaI and HincII, and products for the double-exon and single-exon minigenes were quantified as previously described (10). Quantification of the splice site mutant constructs was done as previously described (4), and for comparison, the total percentage of products with exon IIIb or the total percentage of products with exon IIIc was determined by adding the percentage of double-inclusion products to either the percentage of single-inclusion IIIb products or the percentage of single-inclusion exon IIIc products.

Antibodies and Western blots. Cells were harvested by scraping and resuspended in PBS. Cells were lysed in SDS (0.5% final concentration) in the presence of Complete protease inhibitor (Roche). The total protein concentration was determined by BCA assay (Pierce), and equivalent amounts of protein were run on a 12.5% acrylamide Laemmli gel. Proteins were transferred onto a membrane, and a Western blot assay was performed using standard techniques. The following antibodies were used for the detection of protein bands: anti-Flag M2 monoclonal antibody (Sigma), anti-V5 monoclonal antibody (Invitrogen), anti-CA150 antiserum, anti-polypyrimidine tract-binding protein antiserum, anti-hnRNP F/H H-300 antiserum (Santa Cruz), anti-hnRNP F N-15 antiserum (Santa Cruz), and anti-hnRNP H antiserum (15).

Bioinformatic analyses. Alignment of amino acid sequences for hnRNP H1, hnRNP H2, hnRNP F, hnRNP H3a, and hnRNP H3b was done using the MacVector 6.5.3 ClustalW alignment tool with the default settings. Exonic splicing enhancer sequences were predicted using ESEFinder 3.0 with the default matrix score thresholds (12, 32).

Coimmunoprecipitation experiments. Coimmunoprecipitation of Flag-tagged proteins was done as follows. HEK293T cells (300,000 cells) were seeded into each well of a six-well plate in 2.0 ml of medium without antibiotics. The cells were transfected 24 h later. Two micrograms of both expression plasmids was diluted to 250 μl with OptiMEM and then mixed with 10 μl of Lipofectamine 2000 (Invitrogen) diluted to 250 μl with OptiMEM. After 20 min of incubation, the reagent was gently added to the cells. Cells were grown for 48 h and harvested in PBS by scraping. Cells were spun down at 500 × *g* for 5 min and resuspended in lysis buffer (50 mM Tris-HCl [pH 7.4], 150 mM NaCl, 1 mM EDTA, 1.0% Triton X-100). Immunoprecipitation (IP) of proteins was done as follows. Cell lysates were spun down at 20,000 × *g* for 10 min, and the cell lysate was removed and diluted with 500 μl of binding buffer (50 mM Tris-HCl [pH 7.6], 150 mM NaCl, 0.01% NP-40). Samples of the cell lysates were removed at this point and added to SDS-polyacrylamide gel electrophoresis (PAGE) loading buffer. Lysates were then agitated overnight at 4°C with 50 μl of M2 anti-Flag affinity agarose (Invitrogen). The agarose was spun down at 2,000 × *g* for 5 min, and the pellet was washed in 1,000 μl of wash buffer (50 mM Tris-HCl [pH 7.6], 150 mM NaCl, 1.0% NP-40), agitated for 5 min at 4°C, and spun down at 2,000 × *g* for 5 min. Precipitated proteins were extracted by boiling in 1× SDS-PAGE loading buffer. Cell lysates and precipitated proteins were run on 12.5% SDS-PAGE gels, and Western blot analyses were performed to determine protein levels in each sample.

Nuclear extracts. Large-scale HeLa nuclear extracts were prepared as previously described (18). Small-scale nuclear extracts were prepared from cells overexpressing tagged proteins as follows. HEK293T cells (300,000 cells) were seeded into each well of a six-well plate in 2.0 ml of medium without antibiotics. The cells were transfected 24 h later. A total of 1.0 μg of either pTracer or pTracer Fox 2 and a total of 3.0 μg of p3F-H1 and/or p3F-ASF (balanced with empty p3xFLAG) were diluted to 250 μl with OptiMEM and then mixed with 10 μl of Lipofectamine 2000 (Invitrogen) diluted to 250 μl with OptiMEM. After 20 min of incubation, the reagent was gently added to the cells. Cells were grown for 48 h, trypsinized, and split into a T-150 flask. The T-150 flask was grown to 80% confluence, and cells were harvested in PBS by scraping. Cells were spun down for 10 min at 500 × *g*, and nuclear extracts were prepared from cell pellets. The nuclear extracts were prepared using a modified Dignam protocol in which the glass douncing the solutions was replaced by moving the solution through an 18-gauge needle in order to lyse the swollen cells and break up the nuclear pellet (18).

UV-cross-linking and IP assay. Radiolabeled RNA was in vitro transcribed from pT73C linearized with HindIII with T7 RNA polymerase (Invitrogen) according to the protocol provided by the manufacturer using [α-^{32}P]UTP (Perkin-Elmer). RNA was purified by extraction with phenol-chloroform-isoamyl alcohol, followed by ethanol precipitation according to standard techniques.

Nuclear extracts were spun down at 20,000 × *g* for 15 min to remove precipitated proteins, and cross-linking reaction mixtures were assembled as follows. Cross-linking reaction mixtures were composed of 600,000 cpm of radiolabeled exon IIIc RNA and 10 μl of nuclear extract diluted to 20 μl in minimal binding buffer (with a final concentration of 30 mM HEPES [pH 7.9], 64 mM KCl, and 2 mM $MgCl_2$). The RNA and extracts were incubated at 30°C for 15 min, spun down, and cross-linked on ice with 1000 mJ of ultraviolet radiation in a Stratalinker apparatus (Stratagene). Any remaining RNA was degraded with an RNase cocktail (Invitrogen) through incubation at 37°C for 1 h. Cross-linked proteins were then diluted in coimmunoprecipitation binding buffer, and IP was performed as described above.

RESULTS

hnRNP H and hnRNP F are potent silencers of FGFR2 exon IIIc. Within exon IIIc, just upstream of the exonic UGCAUG Fox binding site, there are three GGG motifs, which could recruit hnRNP H and hnRNP F proteins to the exon. In order to determine if hnRNP H1 had a role in the silencing of FGFR2 exon IIIc, we overexpressed a Flag-tagged version of hnRNP H1 with a minigene that reports on exon IIIc splicing in HEK293T cells (4), which normally express FGFR2 IIIc (Fig. 2A). Protein levels of Flag-tagged hnRNP H1 were detected in a Western blot assay using an anti-Flag tag antibody (Fig. 2B). The splicing response to overexpression was determined by semiquantitative RT-PCR analysis of the minigene reporter products. Consistent with previous findings, the HEK293T cells included exon IIIc very efficiently; however, we observed a dose-dependent decrease in exon IIIc inclusion with increasing amounts of hnRNP H1 (Fig. 2C and D). Levels of exon IIIc inclusion were reduced from nearly 100% inclusion to ~20% inclusion. At the two higher doses of hnRNP H1 plasmid, the major splicing product from the minigene was the skipped product (U-D), where the flanking U and D exons are joined to each other. These data demonstrated that hnRNP H1 could function as a potent silencer of exon IIIc splicing.

Given the high level of homology between members of the hnRNP H subfamily of proteins (hnRNP H1, H2, H3, and F), we asked whether two other members, hnRNP F and hnRNP H3, could also silence exon IIIc. We did not assay the activity of hnRNP H2 because the amino acid sequence differs from that of hnRNP H1 by only 10 residues. In order to assay their silencing activities, hnRNP F and hnRNP H3 were cloned into the same Flag expression vector as hnRNP H1 and overexpressed in HEK293T cells. We chose a dose of hnRNP H1 that would result in about the 50% inclusion of exon IIIc to best compare the relative effect of the different proteins. Several doses of each plasmid were transfected into HEK293T cells. Plasmid doses that resulted in similar protein levels, as determined by a Western blot assay for the common protein tag, were compared (Fig. 2E). As expected, the overexpression of hnRNP H1 caused a decrease in the minigene products that included exon IIIc (Fig. 2F). Over the course of multiple experiments, we observed that hnRNP H1 and hnRNP F silenced exon IIIc to nearly the same extent when overexpressed to similar levels. hnRNP H3 displayed an ability to silence exon IIIc that was about half that of hnRNP H1 and hnRNP F. We also found that both annotated human isoforms, hnRNP H3a and hnRNP H3b, had similar levels of activity (data not shown). Since the difference between H1, F, and H3 is that the latter does not have RRM1, these results suggested that the RRM1 domain of hnRNP H1 could play a role in allowing hnRNP H1 and hnRNP F to silence exon IIIc to a greater extent than hnRNP H3. This was tested and confirmed by the structure-function analysis of hnRNP H1 described below.

In order to determine if the effect the we observed with the overexpression of hnRNP H1 was direct, we created three different substitution mutations within the region of exon IIIc. These substitution mutations span the GGG motifs in the mutant minigene splicing reporters, called pI12-DE-Mut1, pI12-DE-Mut2, and pI12-DE-Mut3 (Fig. 3A). Flag-hnRNP H1 and one of the three different minigenes were cotransfected

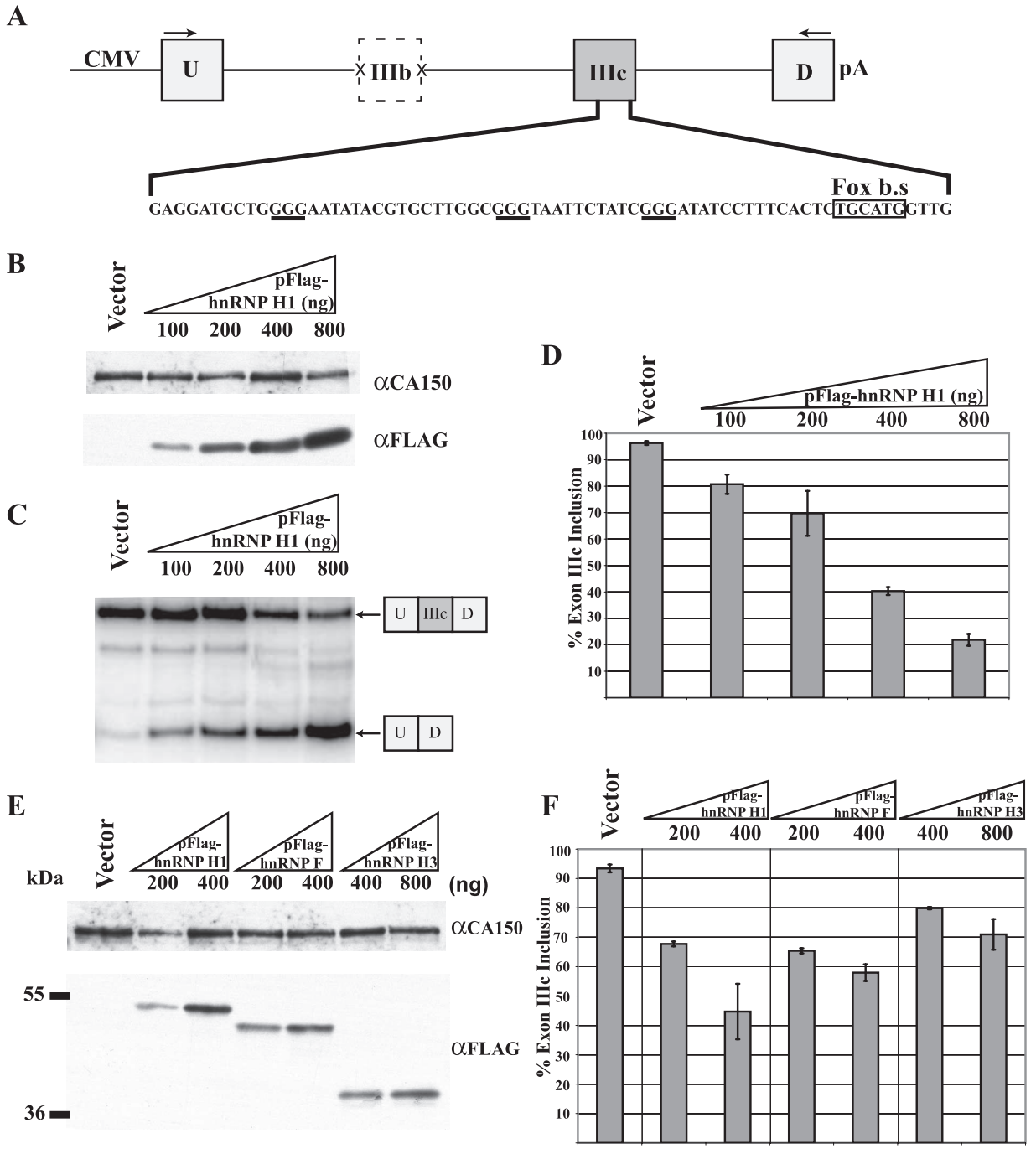

FIG. 2. Silencing of FGFR2 exon IIIc by members of the hnRNP H/F family. (A) Schematic diagram of the minigene that reports on the inclusion of FGFR2 exon IIIc. Functional exons are represented by labeled solid boxes. The cytomegalovirus (CMV) promoter and polyadenylation signal are noted, along with the region within the flanking adenovirus exons that anneals to the PCR primers used to amplify the minigene products. The exon IIIb splice sites were mutated, and the exon was not included under any condition (dashed box). The WT sequence within exon IIIc has been expanded to show the GGG motifs (black bars) and Fox binding (box). (B) Western blot showing the overexpression of Flag-tagged hnRNP H1. Protein overexpression was shown by detection with an antibody directed against the Flag tag. Loading in the lanes was controlled by the detection of the CA150 protein. (C) Gel showing the products of the minigene as amplified by RT-PCR using primers specific to the U and D exons. The bands, which represent the U-IIIc-D and U-D spliced products, are indicated by arrows. (D) Percentage of reporter transcripts including exon IIIc as determined by RT-PCR. Columns indicate the average of triplicate wells transfected with the indicated plasmids at the indicated amounts. Bars show standard deviations between the individual wells. (E) Western blot showing the overexpression of Flag-tagged hnRNP H1, hnRNP F, and hnRNP H3. Protein overexpression was shown by detection with an antibody directed against the Flag tag. Loading in the lanes was controlled by the detection of the CA150 protein. (F) Percentage of reporter transcripts including exon IIIc as determined by RT-PCR. Columns indicate the averages of triplicate wells transfected with the indicated plasmids at the indicated amounts. Bars show standard deviations between the individual wells.

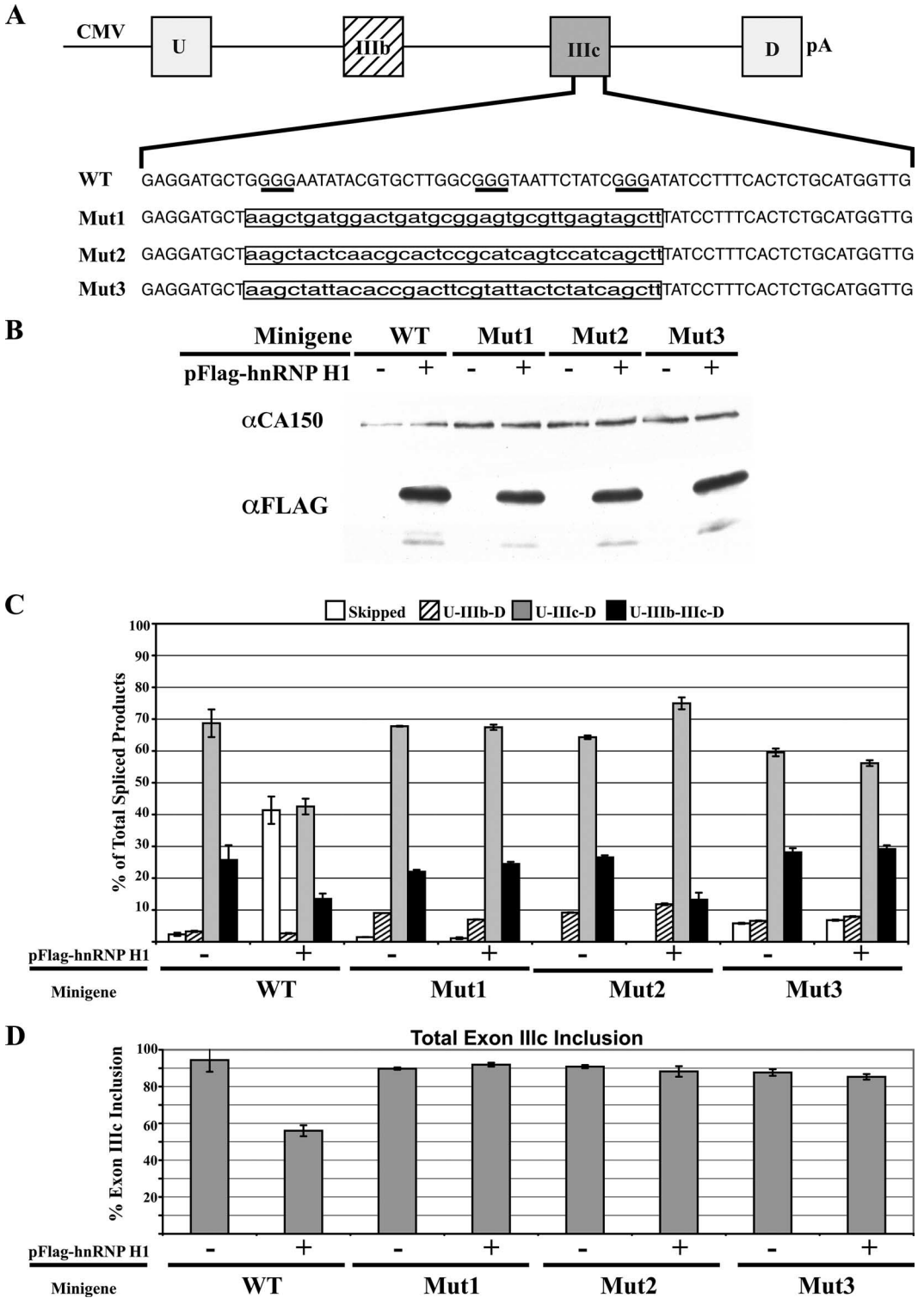

FIG. 3. Silencing of FGFR2 exon IIIc induced by hnRNP H1 overexpression required GGG motifs within exon IIIc. (A) Schematic diagram of a panel of mutant double-exon minigene reporters. The region within exon IIIc, which has been mutated, has been expanded to show the nucleotide sequence. The mutant minigenes have the nucleotide changes denoted by lowercase letters, which are boxed. The hnRNP H/F minimum binding site, GGG motifs, are underlined with thick black bars. CMV, cytomegalovirus. (B) Western blot showing the overexpression of Flag-tagged hnRNP H1. Protein overexpression was shown by detection with an antibody directed against the Flag tag. Loading in the lanes was controlled by detection of the CA150 protein. (C) Minigene spliced products as determined by RT-PCR. Columns indicate average amounts of each spliced product when the indicated minigenes were cotransfected into HEK293T cells in triplicate wells with the indicated expression plasmids. The splicing product that each column represents is indicated at the top of the graph. Bars show standard deviations between the individual wells. (D) The percentage of transcripts that include exon IIIc was calculated by adding the percentage of U-IIIc-D and U-IIIb-IIIc-D transcripts. Bars represent errors in the form of standard deviations, which were propagated through the calculations.

into HEK293 cells to determine if the silencing of exon IIIc by hnRNP H1 depended on this region of the exon (Fig. 3B). In order to best observe differences between the reporters, we chose a dose of pFlag-hnRNP H1 that we knew would inhibit exon IIIc inclusion to approximately 50%. This level of silencing is in the middle part of the dose response to hnRNP H1 overexpression and would allow us to notice both more and less potent silencing activities. In HEK293T cells, the major spliced product of the minigene, which reports on the splicing of both exon IIIb and exon IIIc, was single-inclusion exon IIIc (U-IIIc-D), but some double inclusion (U-IIIb-IIIc-D) was observed (Fig. 3C). Consistent with the results obtained from the single-exon minigene, the overexpression of pFlag-hnRNP H1 led to the silencing of exon IIIc in the wild-type (WT) construct, which is seen as an increase in the levels of the skipped product (U-D). In contrast, all three mutants that lacked the three GGG motifs were insensitive to similar levels of hnRNP H1 overexpression (Fig. 3C and D). This strongly suggests that hnRNP H1 silenced exon IIIc by binding the GGG motifs within the exon.

Either hnRNP H or hnRNP F is required for silencing FGFR2 exon IIIc. Given the previous data that indicate that hnRNP H1 and hnRNP F could silence exon IIIc when overexpressed, we wanted to determine whether hnRNP H and hnRNP F were necessary for the silencing of FGFR2 exon IIIc. We used siRNA duplexes to deplete each protein individually or both proteins together. In order to address concerns about off-target effects, we used pools of duplexes to target each protein and followed this by the verification of our results with two individual duplexes from the pool. The experiment was done in DT cells, where exon IIIc is efficiently silenced. hnRNP H and hnRNP F expression levels were reduced by the transfection of DT cells with siRNA duplexes at a final concentration of 20 nM, and this reduction was confirmed by Western blot assays (Fig. 4B). All siRNA treatments were effective at reducing the protein levels of the targeted protein by at least 10-fold, and the identity of each of the protein bands observed by the Western blotting was verified by at least two different antisera (Fig. 4B and data not shown). Interestingly, when hnRNP F was reduced by siRNA, levels of hnRNP H increased, whereas a reciprocal effect was not observed upon the depletion of hnRNP H. The control C2 duplex, which has no known mRNA targets and did not alter the levels of hnRNP H or hnRNP F, did not alter the silencing of exon IIIc. RNAi depletion of either hnRNP H or hnRNP F alone resulted in either no increase in exon IIIc inclusion or a small increase in exon IIIc inclusion dependent upon which duplex, or set of duplexes, was used (Fig. 4C). When hnRNP H and hnRNP F are depleted together, however, we saw greater-than-twofold increases in exon IIIc inclusion from the minigene (Fig. 4C). The knockdown of both proteins resulted in an increase to almost 80% exon IIIc inclusion. The results obtained using pools of duplexes to hnRNP H and hnRNP F were confirmed using two sets of individual duplexes to hnRNP H and hnRNP F. These results demonstrate that the efficient silencing of FGFR2 exon IIIc requires either hnRNP H or hnRNP F and that the two proteins are functionally redundant with respect to their functions as splicing silencers.

Disruption of silencing due to knockdown of hnRNP H and hnRNP F requires GGG motifs. As shown above, we demonstrated that the silencing of exon IIIc in HEK293T cells by the overexpression of hnRNP H required the exonic region that contained three GGG motifs. This type of experiment provides strong evidence that the effect observed was mediated directly by the interaction of that protein with the RNA. We also wanted to demonstrate that the effect upon the knockdown of hnRNP H and hnRNP F that we saw was dependent upon these motifs. The problem was that if the silencing of exon IIIc required the recruitment of hnRNP H and/or hnRNP F to the exon, the mutation of the GGG motifs would disrupt the silencing of the exon similarly to the siRNA depletion of both proteins. Nonetheless, studies have recently shown that a variety of RNA sequences can function as splicing silencers (36), and therefore, we wondered whether one of the three mutants in Fig. 3 could serendipitously provide the silencing of exon IIIc in DT cells. We tested Mut1, Mut2, and Mut3 for the ability to silence exon IIIc in DT cells, and indeed, Mut3 gave levels of exon IIIc inclusion similar to that of the WT exon despite lacking any hnRNP H and hnRNP F binding sites. Utilizing Mut3, we tested whether or not the effect observed upon the knockdown of hnRNP H and hnRNP F depended on the region containing the GGG motifs. In DT cells, these minigenes, which contain both exon IIIb and exon IIIc, show mostly exon IIIb single-inclusion products (U-IIIb-D) and have a background amount of the double-inclusion product (U-IIIb-IIIc-D) (Fig. 5B). This results from the efficient inclusion of exon IIIb and the silencing of exon IIIc. We observed that levels of exon IIIc inclusion, which were seen mostly as double-inclusion products (U-IIIb-IIIc-D) in the WT minigene and Mut3 minigene, are nearly identical in the control (C2) samples (Fig. 5B and C). When both hnRNP H and hnRNP F are knocked down, the WT minigene showed a dramatic increase in levels of exon IIIc inclusion, but the Mut3 minigene levels of IIIc inclusion were unaffected (Fig. 5B and C). These results prove that the effect of the siRNA depletion of hnRNP H and hnRNP F depended on the exonic region containing the hnRNP H and hnRNP F binding sites. We believe that the data presented in the last two sections represent the most rigorous study to date indicating that hnRNP H and F are necessary for the silencing of specific exons.

Structure-function analysis of hnRNP H1. The data obtained when we overexpressed hnRNP H3 hinted that RRM1 in both hnRNP H1 and hnRNP F could play a role in efficiently silencing exon IIIc. To test this and to elucidate the importance of other motifs in hnRNP H and hnRNP F function, we performed a structure-function analysis on hnRNP H1. We expressed a panel of hnRNP H1 mutants in HEK293T cells (Fig. 6A and B). In order to compare the abilities of the proteins to silence exon IIIc, we normalized the change in exon IIIc inclusion by dividing the change in the percentage of exon IIIc inclusion by the change that we saw with the overexpression of pFlag-hnRNP H1-WT (Fig. 6D). We found that the deletion of the C-terminal 160 amino acids, MutΔ and Mutγ, had no impact on the silencing activity of the protein. This dispensable region accounts for more than the last one-third of the protein including the highly conserved RRM3 and an extensive glycine-rich region (Fig. 6A). Additionally, we also determined that the amino-terminal 12 amino acids were not required, and in fact, Mutα, which lacks these, appeared to silence exon IIIc slightly better than did the WT protein. In contrast, if we

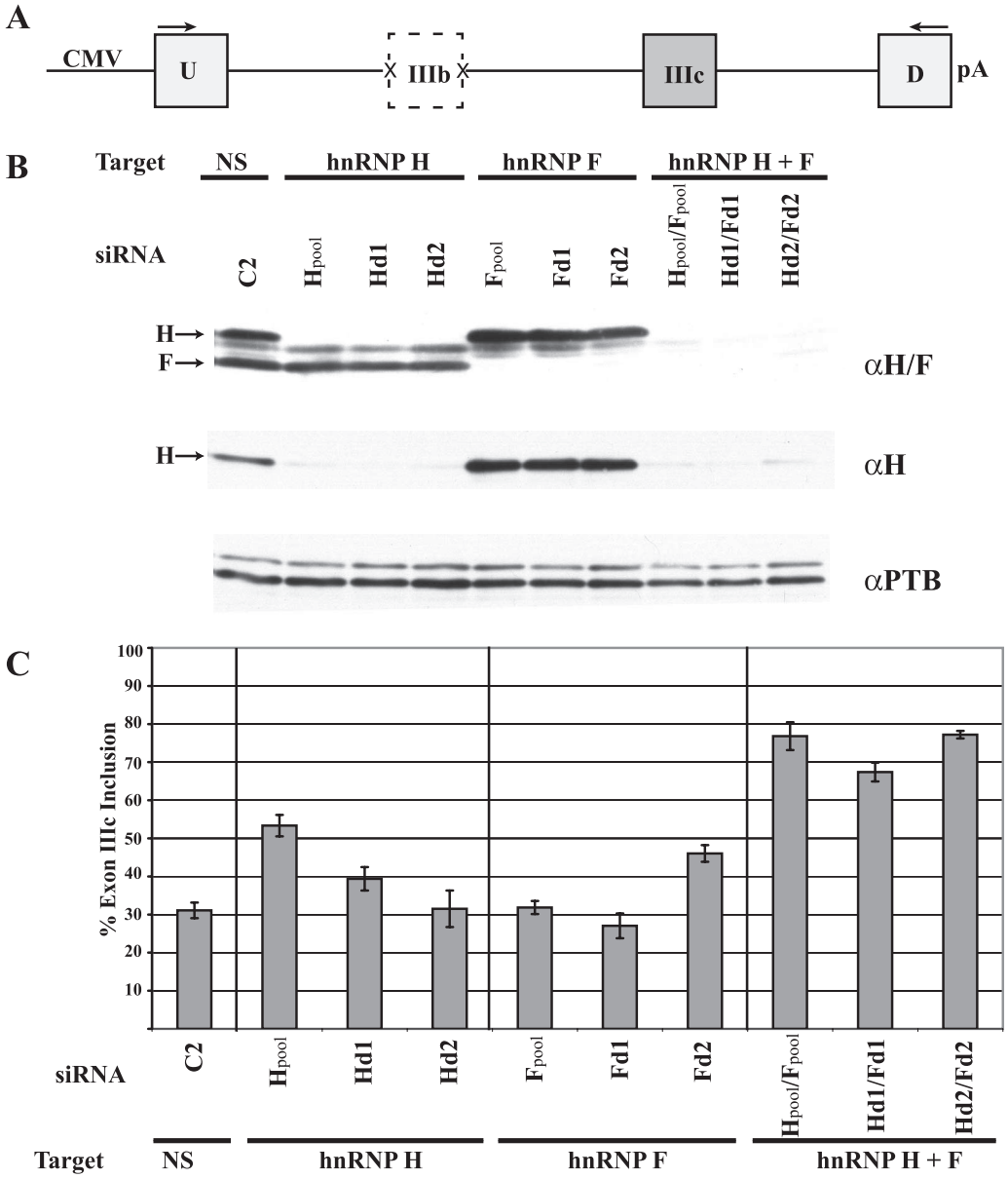

FIG. 4. RNAi-mediated depletion of both hnRNP H and hnRNP F disrupted silencing. (A) Schematic diagram of the minigene that reports on the inclusion of FGFR2 exon IIIc. CMV, cytomegalovirus. (B) Western blots showing effect of transfection of DT cells with siRNA duplexes targeting hnRNP H, hnRNP F, or both. Duplex C2 (NS), which has no known mRNA target, was used as a control. The blots show the results of the following transfections: transfection with a pool of four different duplexes against hnRNP H (H_{pool}), transfection with duplex 1 (Hd1) and duplex 2 (Hd2) of the hnRNP H pool, transfection of three duplexes against hnRNP F (F_{pool}), transfection with duplex 1 (Fd1) and duplex 2 (Fd2) of the hnRNP F pool, transfection with a combination of duplex pools for H and F, transfection with a combination of duplex 1 for H and F, and transfection with a combination of duplex 2 for H and F. Protein levels were determined by Western blots with antibodies to hnRNP H and hnRNP F and the hnRNP H carboxy terminus, and PTB was used as a loading control. An increase in levels of hnRNP H was observed when hnRNP F was knocked down. We believe that this increase may be caused by a relief of autoregulation where hnRNP H and hnRNP F proteins silence exon 4 of the HNRPH1 gene (D. M. Mauger and M. A. Garcia-Blanco, unpublished observation). (C) Percentage of reporter transcripts including exon IIIc as determined by RT-PCR. Columns indicate the averages of triplicate wells transfected with the indicated siRNA. Bars show standard deviations between the individual wells.

disrupted either of the first two RRMs, the protein lost the ability to effectively silence exon IIIc. The deletion of the first 86 amino acids in Mutβ that remove RRM1 reduced the ability of the protein to silence exon IIIc by over fivefold, representing a nearly complete disruption in the silencing activity of the protein. Alanine substitutions of residues believed to contact RNA, W20 and Y82 in RRM1 (Flag-R1AA) or F120 and Y180 in RRM2 (Flag-R2AA), also abrogated the silencing of exon IIIc (Fig. 6D). It is interesting that the double amino acid substitution in RRM1, R1AA, did not disrupt the activity of the protein to the same extent as the deletion of the domain, Mutβ, or the double amino acid substitution in RRM2. R1AA

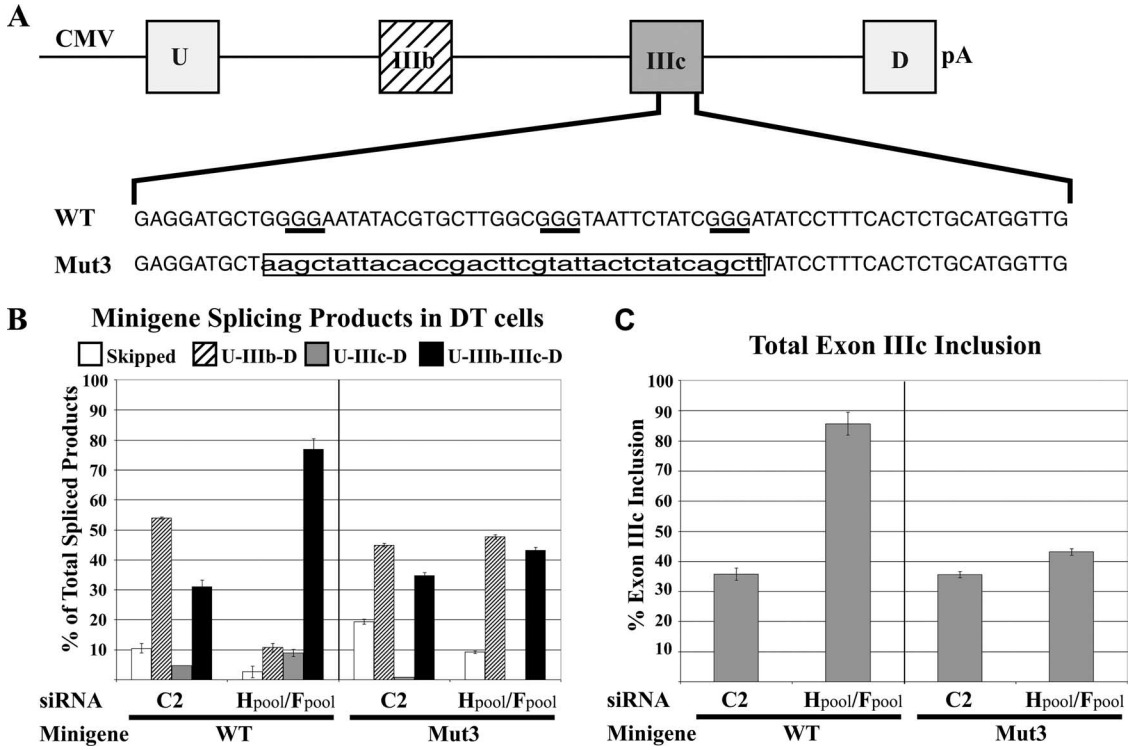

FIG. 5. A novel mutant revealed that the effect of knocking down hnRNP H and hnRNP F required GGG motifs within FGFR2 exon IIIc. (A) Schematic diagram of a panel of mutant double-exon minigene reporters. The region within exon IIIc, which has been mutated, has been expanded to show the nucleotide sequence. The mutant minigene has the nucleotide changes denoted by lowercase letters, which were boxed. The hnRNP H/F minimum binding site, GGG motifs, are underlined with thick black bars. CMV, cytomegalovirus. (B) Minigene spliced products of the minigenes in DT cells as determined by RT-PCR. Columns indicate average amounts of each spliced product when the indicated minigenes were transfected into DT cells that were treated with the indicated siRNA duplexes in triplicate wells. The splicing product that each column represents is indicated at the top of the graph. Bars show standard deviations between individual wells. (C) The percentage of transcripts that include exon IIIc was calculated by adding the percentage of U-IIIc-D and U-IIIb-IIIc-D transcripts. Bars represent the errors in the form of standard deviations, which were propagated through the calculations.

had about one-half of the silencing activity of the WT protein; this was reminiscent of the activity seen with hnRNP H3. Taken together, these results demonstrate that RRM1 and RRM2 were essential for the full silencing activity of hnRNP H. These data indicate that the lack of RRM1 could account for the reduced silencing activity seen with hnRNP H3.

In order to expand upon our initial series of deletions, we created three sequential deletions of the region between RRM2 and RRM3 referred to as MutC1, MutC2, and MutC3 (Fig. 6A). All three of these deletions severely disrupted the ability of the protein to silence exon IIIc, similarly to that seen when the second RRM is mutated (Fig. 6E and F). Immunofluorescence against the Flag tag revealed that all of the mutants, with the exception of MutC2 and MutC3, were localized to the nucleus (data not shown). These data suggest that in addition to a nuclear localization sequence, the region between RRM2 and RRM3 contains an element critical to the silencing function of hnRNP H1. Just what this element could be will be addressed later in the paper. Furthermore, in sharp contrast to the findings of structure-function analyses of the hnRNP A1 protein, the carboxy-terminal glycine-rich region was completely dispensable for silencing activity within hnRNP H1. These differences suggest that hnRNP H1 can silence exons by a distinct mechanism.

GGG motifs function as exonic splicing silencers that antagonize an exonic splicing enhancer to control exon IIIc inclusion. The analysis described above suggested that the binding of hnRNP H1 would be sufficient to silence exon IIIc and that the region of exon IIIc containing the GGG motifs was required for this silencing. In order to further dissect this exonic region, we constructed several mutant minigenes and determined the effect that the mutations had on the inclusion of exon IIIc in DT cells, which normally silence this exon. We constructed these mutations in the background of pI-12-DE, which has fully functional exons IIIb and IIIc. pI-12-DE-Mut1 and pI-12-DE-Mut2, which were described above, disrupted H and F binding sites, and this led to increased levels of exon IIIc inclusion, while exon IIIb inclusion was unaffected (Fig. 7B). Since these constructs contained both of the FGFR2 exons, the increase in exon IIIc inclusion was manifested as an increase in the product that includes both exon IIIb, which is activated in DT cells, and exon IIIc (U-IIIb-IIIc-D) (Fig. 7B). The total level of transcripts including exon IIIc was calculated by adding together the double-inclusion product and the exon IIIc-only product. Both Mut1 and Mut2 display over a twofold increase in the total level of exon IIIc inclusion (Fig. 7C).

In order to refine our analysis, we made discrete mutations of the GGG motifs in pI12-DE-Mut4 and pI12-DE-Mut5 (Fig.

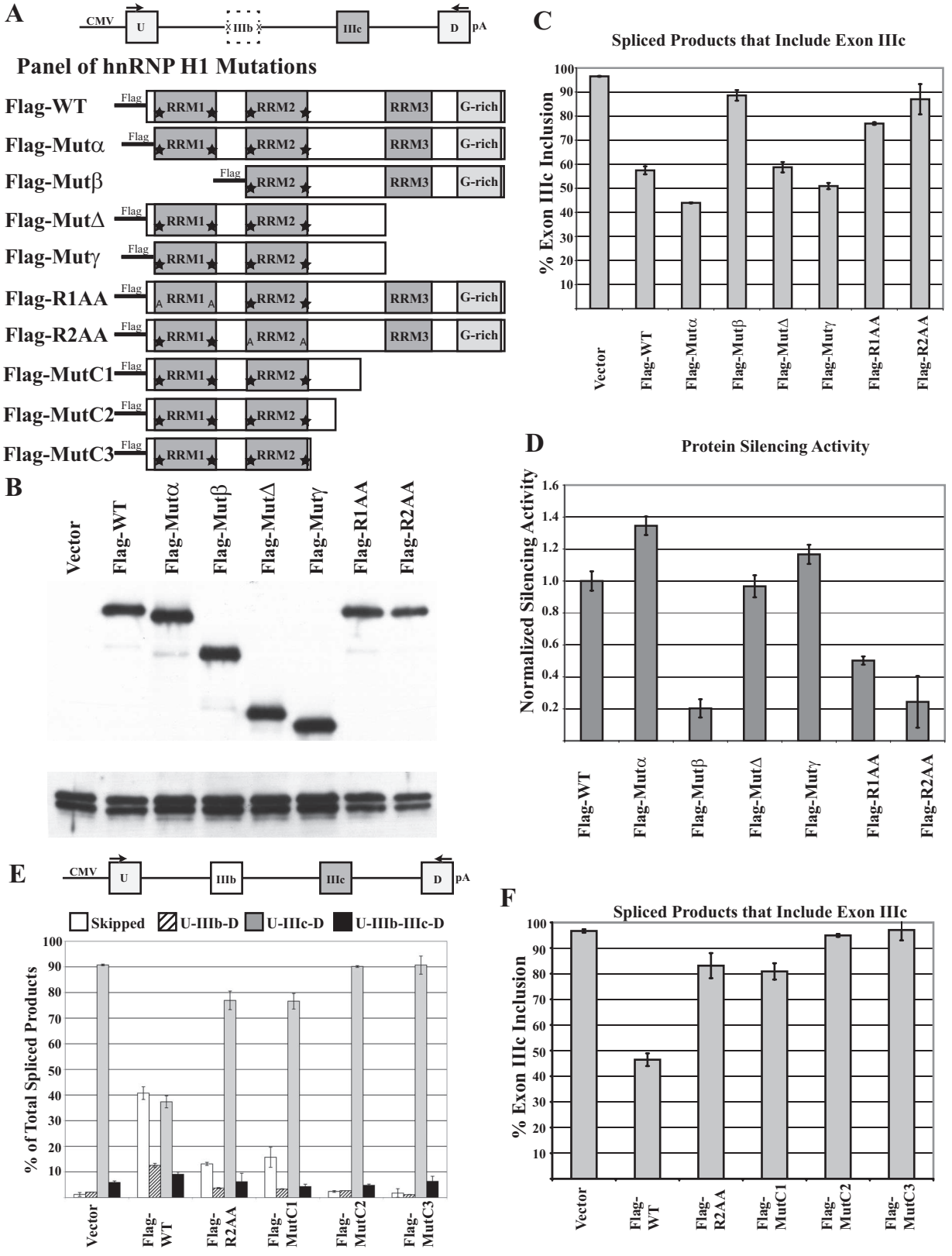

FIG. 6. Mutational analysis of the domains required for the exonic silencing function of hnRNP H1. (A, top) Schematic diagram of the minigene that reports on the inclusion of FGFR2 exon IIIc. CMV, cytomegalovirus. (Bottom) Scaled alignment of the panel of mutants expressed. Annotated domains are indicated by gray boxes, and stars represent amino acids W20, Y82, F120, and Y180. The indicated amino acids were mutated to alanine in mutants Flag-R1AA and Flag-R2AA. (B) Western blot showing the overexpression of the panel of hnRNP H1 mutants. Protein overexpression was shown by detection with an antibody directed against the Flag tag. Loading in the lanes was controlled by detection

7A). To our surprise, we observed exactly the opposite effect of what we observed with the previous mutations. In Mut4 and Mut5, the basal levels of exon IIIc inclusion fell to levels below that of the WT minigene, as seen by a reduction in the levels of the double-inclusion product (Fig. 7B and 7C). Instead of being consistent with the disruption of a silencer, this result suggested that we disrupted an enhancer element.

We analyzed the WT and all mutant sequences through the bioinformatics program ESEFinder 3.0 to search for potential binding sites for members of the SR protein family that could function as ESEs (11, 12, 25, 31, 32, 35). The program identified an ASF/SF2 binding site (CUGGGGA) that included the 5′-most GGG motif. Substitutions in both Mut1 and Mut2 had disrupted this site but unintentionally introduced new putative ASF/SF2 binding sites that were predicted to be at least as potent as the one in the WT sequence by ESEFinder matrix score (Fig. 7A; see Tables S1 and S2 in the supplemental material). Mut4 and Mut5 did not have any predicted ASF/SF2 sites in this region. We hypothesized that overlapping ESE and ESS elements could explain all of the data from the mutational analysis. In order to test this hypothesis, we designed two point mutations, which were predicted to specifically disrupt either the hnRNP H binding site or the ASF/SF2 binding site. We specifically disrupted the hnRNP H and hnRNP F binding GGGA motif (the altered nucleotide is underlined) with a C residue at position 2 in pI12-DE-Mut6 (Fig. 7A). This mutation should abolish binding by hnRNP H family members without significantly changing ASF/SF2 binding (see Tables S1 and S2 in the supplemental material). Indeed, Mut6 increased the inclusion of exon IIIc by twofold, while exon IIIb levels were not affected (Fig. 7B and C). Additionally, we created pI12-DE-Mut7, in which we introduced a C-to-T mutation in the exonic sequence CUGGGGA that is predicted to bind ASF/SF2 (Fig. 7A). Mut7 gave a twofold decrease in levels of exon IIIc inclusion (Fig. 7B and C). Taken together, the dramatic differences observed in the two minigenes with single point mutations indicate that the majority of the effects seen in the above-described mutants can be attributed to the disruption of juxtaposed ESE and ESS sequences within exon IIIc. These data suggest a mechanism by which hnRNP H and hnRNP F silence exon IIIc by directly competing with ASF/SF2 for binding to this overlapping element.

ASF/SF2 antagonizes hnRNP H and hnRNP F to promote exon IIIc inclusion. In order to determine whether ASF/SF2 can antagonize hnRNP H and hnRNP F, we asked if additional ASF/SF2 could rescue exon IIIc inclusion in cells where Flag-hnRNP H1 was overexpressed. We induced the silencing of exon IIIc by overexpressing Flag-tagged hnRNP H in HEK293T cells. These cells were also cotransfected with increasing amounts of pFlag-ASF, which contained the coding sequence of ASF/SF2 cloned into the same vector using the exact same sites as those with pFlag-H1. We detected protein overexpression by Western blotting for the Flag tag, thus allowing a direct comparison of levels of H overexpression to that of ASF/SF2 (Fig. 8B). Our Western blot analysis revealed that the overexpressed ASF/SF2 was posttranslationally modified, as it runs as two distinct bands, which was consistent with previous findings that ASF/SF2 is phosphorylated (37). When cells were transfected with 300 ng of pFlag-H1, levels of exon IIIc inclusion decreased to about 50% (Fig. 8C and D); however, cotransfection with as little as 150 ng of pFlag-ASF completely restored exon IIIc inclusion back to levels seen without the expression of H1 (Fig. 8C and D). It is worth noting that ASF/SF2 also increased levels of exon IIIb inclusion to 30%, about a threefold increase, suggesting a role for ASF/SF2 in exon IIIb inclusion. These results show that ASF/SF2 can functionally antagonize hnRNP H and hnRNP F to activate exon IIIc. The mutational analysis suggests that ASF/SF2 can antagonize hnRNP H and hnRNP F binding by competing for binding to an element that contains overlapping binding sites for these proteins.

hnRNP H, hnRNP F, and ASF/SF2 compete for binding to exon IIIc, a process that is affected by Fox proteins. The above-described data strongly suggest that hnRNP H and hnRNP F silence exon IIIc by competing with ASF/SF2 for binding to the exon. In order to examine this competition further, we performed in vitro binding studies for both hnRNP H1 and ASF/SF2. First, we used a combination of UV cross-linking and IP to verify that the proteins could bind to exon IIIc RNA. Proteins from HeLa nuclear extracts were cross-linked by UV radiation to radiolabeled RNA containing the sequence of exon IIIc. The proteins were then immunoprecipitated using either a rabbit polyclonal antiserum against hnRNP H1 or a monoclonal antibody against ASF/SF2 (Zymogen). The antibody to hnRNP H1 brought down a protein of the expected size that strongly cross-links to exon IIIc, verifying that hnRNP H1 can bind directly to exon IIIc (Fig. 9A). We were not able to demonstrate cross-linking of ASF/SF2 using monoclonal antibody, which could be explained by the poor affinity of this antibody to the cross-linked RNA-protein complex. We addressed this issue in the next experiment.

Next, we sought to determine whether hnRNP H and ASF/

of the PTB protein. (C) Percentage of reporter transcripts including exon IIIc as determined by RT-PCR. Columns indicate the averages of data from triplicate wells transfected with the indicated plasmids. Bars show standard deviations between the individual wells. (D) Relative silencing activity of transfected plasmid compared to silencing observed with transfection of pFlag-H1-WT. The observed silencing activity for each transfection was determined by the difference between the average of the individual transfections and the average of the vector-only control. These differences were normalized such that the difference between the transfection of pFlag-H1-WT and the vector-only control was set to 1.0. Bars represent the error in the form of the standard deviation, which was propagated through the calculations. (E) Schematic diagram of the minigene that reports on the inclusion of FGFR2 exons and minigene spliced products as determined by RT-PCR. Columns indicate average amounts of each spliced product when the minigenes were cotransfected into 293T cells with the indicated expression construct in triplicate wells. The splicing product that each column represents is indicated at the top of the graph. Bars show standard deviations between individual wells. (F) Normalized levels of exon IIIc inclusion for minigenes. The percentage of transcripts including exon IIIc, which includes both U-IIIc-D and U-IIIb-IIIc-D, were normalized to the percentage of exon IIIc in the WT minigene for a given experiment. Bars represent errors in the form of standard deviations, which were propagated through the calculations.

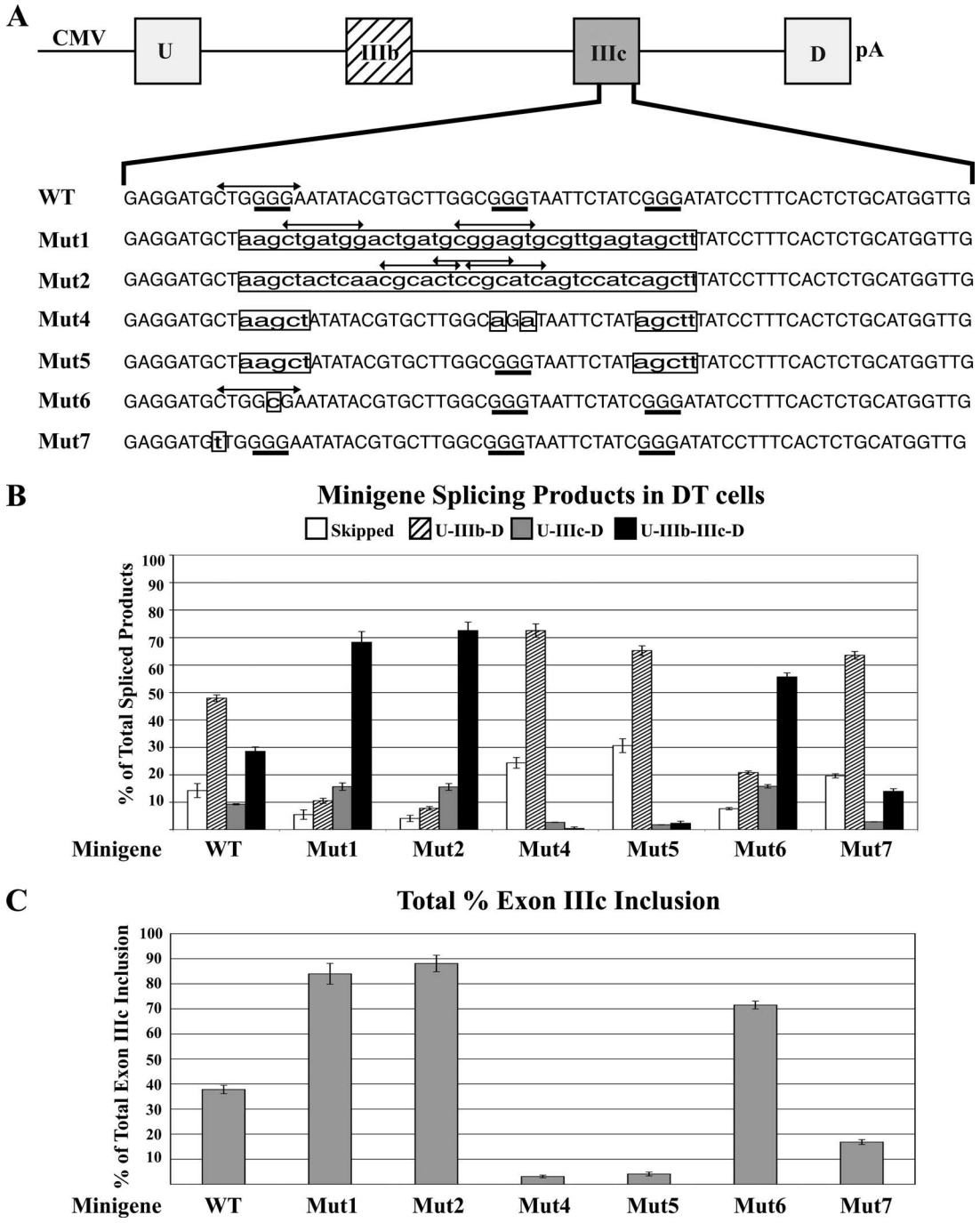

FIG. 7. Mutational analysis of the region within exon IIIc revealed overlapping ESS and ESE. (A) Schematic diagram of a panel of mutant double-exon minigene reporters. The region within exon IIIc, which has been mutated, has been expanded to show the nucleotide sequence. The mutant minigenes have the nucleotide changes denoted by lowercase letters, which are boxed. The hnRNP H/F minimum binding site, GGG motifs, are underlined with thick black bars. Predicted ASF/SF2 binding sites, as determined by ESEFinder 3.0, are indicated by double-headed arrows above the sequence. CMV, cytomegalovirus. (B) Minigene spliced products as determined by RT-PCR. Columns indicate average amounts of each spliced product when the indicated minigenes were transfected into DT cells in triplicate wells. The splicing product that each column represents is indicated at the top of the graph. Bars show standard deviations between the individual wells. (C) Normalized levels of exon IIIc inclusion for minigenes. The percentage of transcripts including exon IIIc, which includes both U-IIIc-D and U-IIIb-IIIc-D, were normalized to the percentage of exon IIIc in the WT minigene for a given experiment. Bars represent errors in the form of standard deviations, which were propagated through the calculations.

SF2 compete for binding to exon IIIc. Traditionally, these competition experiments are done in vitro using proteins expressed and purified from bacteria. Given the posttranslational modifications seen with ASF/SF2, in addition to the ability of SR and hnRNP proteins to bind cooperatively, we chose to do our binding experiments in the context of nuclear extracts prepared from cells overexpressing tagged versions of hnRNP H1 or ASF/SF2. HEK293T cells were transfected with plas-

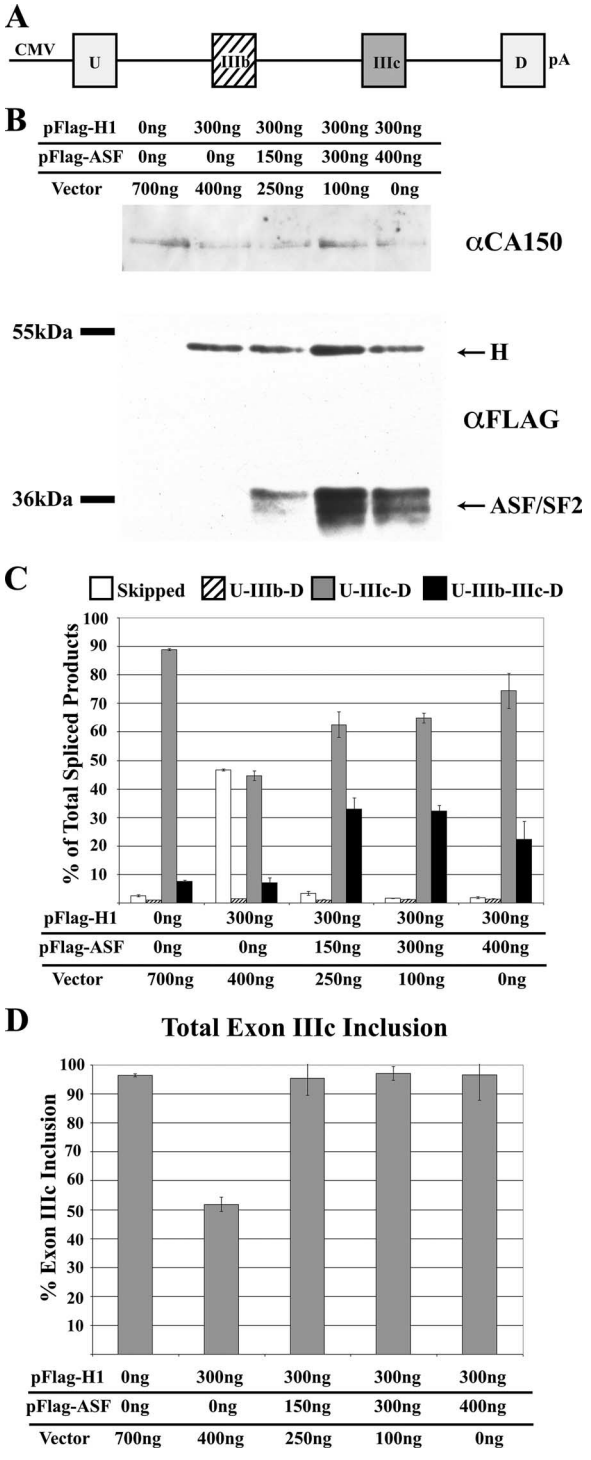

FIG. 8. Overexpression of ASF/SF2 rescued inclusion of exon IIIc in cells where hnRNP H1 was overexpressed. (A) Schematic diagram of the minigene that reports on inclusion of FGFR2 exon IIIc. CMV, cytomegalovirus. (B) Western blot showing overexpression of Flag-tagged hnRNP H1 and/or Flag-tagged ASF/SF2. Protein overexpression was shown by detection with an antibody directed against the Flag tag. The sizes and locations of protein standards are given by labeled black bars, and the expected sizes of full-length hnRNP H and ASF/SF2 are indicated by arrows. Loading in the lanes was controlled by detection of the CA150 protein. (C) Minigene spliced products determined by RT-PCR. Columns indicate average amounts of each spliced product when the indicated minigenes were cotransfected into HEK293T cells in triplicate wells with the indicated expression plasmids. The splicing product that each column represents is indicated at the top of the graph. Bars show standard deviations between the individual wells. (D) The percentage of transcripts that include exon IIIc was calculated by adding the percentage of U-IIIc-D and U-IIIb-IIIc-D transcripts. Bars represent errors in the form of standard deviations, which were propagated through the calculations.

mids, which expressed Flag-tagged versions of hnRNP H1 and/or ASF/SF2. These cells were used to prepare nuclear extracts, and the extracts were assayed by Western blotting to confirm that the cellular extracts contained the tagged proteins at similar levels of hnRNP H1 or ASF/SF2 (data not shown). UV cross-linking assays were used to determine which proteins bound to a radiolabeled RNA containing the exon IIIc sequence, and the Flag-tagged proteins were purified by IP. In order to be certain that the results were indicative of cross-linking and not merely the efficiency of the IP, the affinity resin was kept in excess, and supernatants of all samples were analyzed to make sure no tagged proteins were detectable. Figure 9B shows the results of the cross-linking IP assay. The IP from the extracts transfected with the empty vectors showed background levels of nonspecific cross-linked proteins coming down (Fig. 9B, lane 1). The IP from extracts transfected with either Flag-hnRNP H1 (Fig. 9B, lane 2) or Flag-ASF/SF2 (lane 3) alone showed proteins of the expected sizes cross-linking to the RNA. In the gels pictured in Fig. 9B, hnRNP H appeared as a single band, while ASF/SF2 appeared as a smear. This pattern was similar to what we saw in Western blots for the protein tags. Furthermore, the smeared band in the ASF/SF2 lane hinted that the posttranslational modifications of ASF/SF2 did not create a species of the protein that preferentially binds to exon IIIc in vitro. When hnRNP H1 and ASF/SF2 are coexpressed (Fig. 9B, lane 4), you see dramatically reduced cross-linking of the hnRNP H band and a slight reduction in the intensity of the label in the ASF/SF2 smear were observed, indicating that these proteins compete for cross-linking to the RNA.

Previously, our laboratory showed that cell-type-specific splicing factors belonging to the Fox family could silence the inclusion of FGFR2 exon IIIc (4). In order to determine whether Fox could affect the cross-linking of hnRNP H and ASF/SF2, we prepared nuclear extracts from cells overexpressing Flag-tagged hnRNP H1, Flag-tagged ASF/SF2, and V5-tagged Fox2. We observed that the presence of Fox in these cells, which lack Fox activity, could enhance the cross-linking of hnRNP H in our assay (Fig. 9B, lane 6). We believe that these data demonstrate that hnRNP H1 and ASF/SF2 are in direct competition for in vitro binding to exon IIIc under conditions similar to those seen in the cells during overexpression, and importantly, the presence of Fox2 affects this competition for binding in favor of hnRNP H and hnRNP F binding.

hnRNP H and hnRNP F proteins form a complex with Fox2. Our previous experiment suggested that Fox2 could affect the binding of hnRNP H and hnRNP F to exon IIIc RNA. We performed a coimmunoprecipitation experiment in order to determine if these proteins interacted biochemically. In our first experiment, members of the hnRNP H/F family and sev-

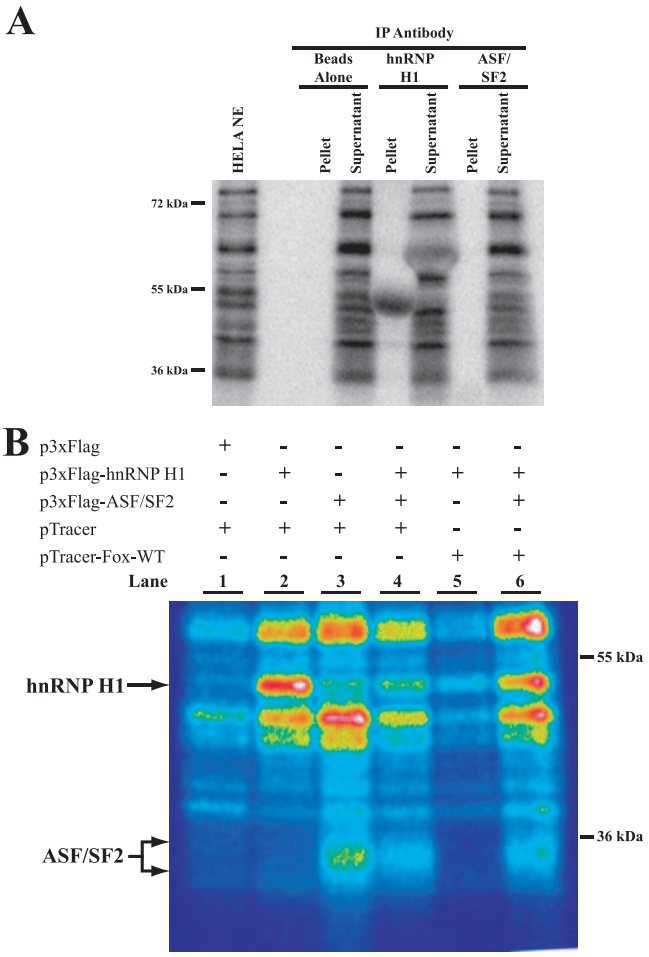

FIG. 9. hnRNP H1 and ASF/SF2 compete for cross-linking to exon IIIc RNA. (A) Gel of the UV cross-linking and IP of hnRNP H1 and ASF/SF2 proteins. Radiolabeled exon IIIc RNA was cross-linked to proteins in HeLa nuclear extract (NE) by UV radiation, and unbound RNA was digested with RNase. The cross-linked proteins were then immunoprecipitated using antibodies against hnRNP H1 and ASF/SF2, run on a gel, and exposed to a phosphor screen to identify labeled proteins. (B) Gel of the UV cross-linking and IP of Flag-tagged hnRNP H1 and ASF/SF2 proteins overexpressed in 293T nuclear preps. Radiolabeled exon IIIc RNA was cross-linked to proteins in the 293T nuclear extract preps by UV radiation, and unbound RNA was digested with RNase. The cross-linked proteins were then immunoprecipitated using antibodies against the Flag tag, run on a gel, and exposed to a phosphor screen to identify labeled proteins. The intensity of the label at different positions within the gel is indicated by a color spectrum that goes in order from least signal to most signal (dark blue, light blue, yellow, orange, red, and white).

eral mutants of hnRNP H1 were overexpressed in HEK293T cells with V5-tagged versions of Fox2. The cells were lysed and used to perform a coimmunoprecipitation for the Flag-tagged proteins. Both the input cell lysates and the immunoprecipitated proteins were run on SDS-PAGE gels, and Western blot assays were done to detect both Flag-tagged and V5-tagged proteins. Figure 10A shows that Fox2 can be precipitated by hnRNP H1 (Fig. 10A, lane 4) and hnRNP F (Fig. 10A, lane 8). Furthermore, these interactions are insensitive to the treatment of the lysates with RNases prior to precipitation. Interestingly, hnRNP H3 (Fig. 10A, lane 9), which lacks the silencing potency of the former two proteins, precipitated less Fox2 than the above-mentioned proteins.

After discovering that hnRNP H, hnRNP F, and Fox proteins could interact, we utilized the panel of mutants from the structure-function analyses of both proteins to map the regions of these proteins required for this interaction. Figure 10A shows the result of the IP of V5-tagged Fox2 by several Flag-tagged mutants of hnRNP H1. Mutβ (Fig. 10A, lane 5), which does not silence exon IIIc as well as the WT, still retained the ability to precipitate with Fox2. MutΔ (Fig. 10A, lane 6), which efficiently silenced exon IIIc, retained the ability to interact with Fox, although the deletion of the carboxy-terminal region did appear to hinder the interaction with Fox compared to full-length protein. In addition to these mutants, we tested MutC1, which contains only the first 260 amino acids of hnRNP H1. This protein was not able to silence exon IIIc (Fig. 6E), and when co-overexpressed with full-length Fox2, the IP of the MutC1 protein (Fig. 10A, lane 7) precipitated very little of the V5-tagged Fox2. These results indicate that at least in the case of Flag-hnRNP-H1-MutC1, there is a correlation between the ability of the protein to associate with Fox and the ability to silence exon IIIc.

In order to confirm the above-described results, we performed IPs for both Flag-tagged hnRNP H1 and a panel of V5-tagged Fox mutants. Figure 10B shows the result of the IP of a panel of V5-tagged mutants of Fox2 by full-length Flag-tagged hnRNP H1. The splicing activities of this panel of mutants was previously reported by our laboratory (4). Once again, the full-length version of Fox and hnRNP H1 interacted (Fig. 10B, lane 1). The Fox Δ2-102 mutant (Fig. 10B, lane 2), which deletes 100 amino acids from the amino terminus of the protein, still retains the ability to silence exon IIIc. This protein still precipitated hnRNP H1, albeit at a lower level than that of the full-length protein. Fox mutant Δ294-377 (Fig. 10B, lane 3) and Fox mutant Δ206-377 (Fig. 10B, lane 4) both contain carboxy-terminal deletions of the Fox2 protein. Both of these proteins lose the ability to silence exon IIIc as well as the ability to precipitate hnRNP H1. These data suggest a functional significance of the interaction of hnRNP H1 and Fox and indicate that the loss of their ability to interact with the hnRNP H and hnRNP F proteins could explain why these mutants can no longer function as silencing factors. In order to verify and support our previous data, we performed another IP experiment, this time for the V5-tagged Fox protein. Fox2-V5-WT and Fox 2-V5-Δ206-377 were overexpressed with full-length Flag-hnRNP H1. Fox2-V5-WT (Fig. 10B, lane 7) but not Fox 2-V5-Δ206-377 (Fig. 10B, lane 8) was able to precipitate full-length Flag-hnRNP H1. Additionally, we performed a Western blot assay for endogenous hnRNP H1. Figure 10B shows that the full-length Fox protein precipitates the endogenous hnRNP H1 in the absence of overexpression of Flag-tagged hnRNP H (Fig. 10B, lane 6). Taken together, these data provide strong evidence for a functionally relevant biochemical interaction between the hnRNP H and hnRNP F proteins and Fox2.

DISCUSSION

In this paper, we establish the hnRNP H/F family of proteins as being splicing regulators of FGFR2 exon IIIc. Our studies

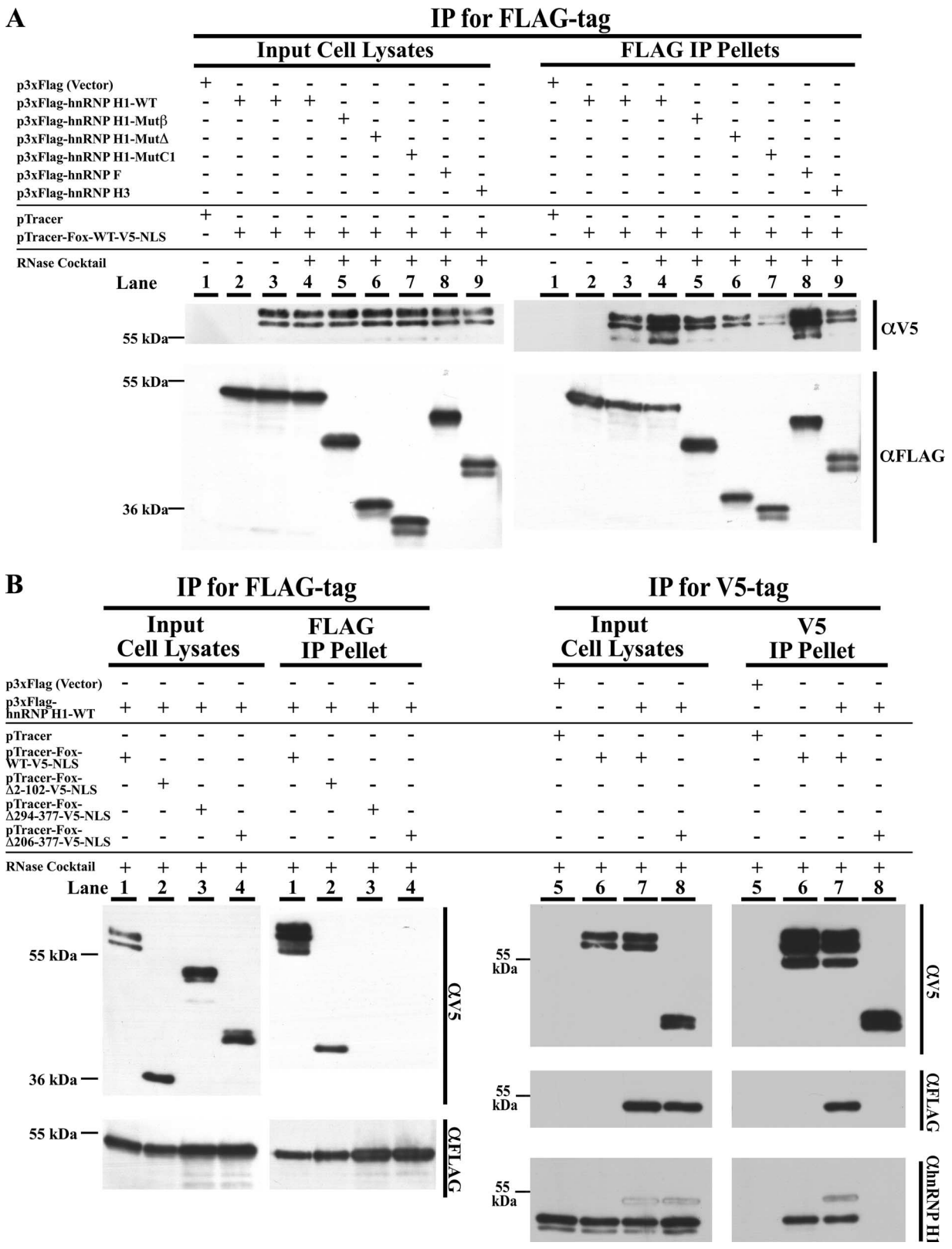

FIG. 10. hnRNP H and hnRNP F proteins immunoprecipitate Fox2. Western blots of the IP reactions for the Flag and V5 tags are shown. 293T cells were transfected with the indicated plasmids, and IPs were performed for the indicated tags. Gels were run to analyze the protein contents of both the input cell lysates and the precipitated pellets, and Western blots were performed to detect tagged proteins or endogenous hnRNP H1. RNase cocktail was added to the cell lysates prior to IP where indicated.

demonstrate that these proteins silence exon IIIc and identify a high-affinity binding site for these proteins located within this exon, which functions as an ESS. Intriguingly, the ESS overlaps an element that functions as an ESE and is predicted to bind the SR protein ASF/SF2. The juxtaposition of the ESS and ESE suggests a simple mechanism of action, where hnRNP H and hnRNP F proteins directly compete with ASF/SF2 for binding to this region of the exon. In support of this mechanism, we show that hnRNP H, hnRNP F, and ASF/SF2 functionally antagonize each other. Furthermore, under conditions similar to those seen in cells when the proteins were overexpressed, we demonstrate that hnRNP H1 and ASF/SF2 will compete with each other for binding to exon IIIc. Taken together, these results conclusively establish hnRNP H and hnRNP F as being repressors of exon IIIc inclusion that function by antagonizing ASF/SF2.

Because hnRNP H, hnRNP F, and ASF/SF2 levels are similar in cells with distinctly different splicing regulations, this competition, in and of itself, could not explain the cell-type-specific splicing pattern. However, the interactions of hnRNP H and hnRNP F with the Fox proteins, which we described here for the first time, provide an elegant way to regulate the activity of hnRNP H and hnRNP F proteins in the context of exon IIIc without having to change the overall protein levels.

This paper provides the first evidence that Fox2 complexes with members of the hnRNP H/F family. We demonstrate that Fox2 can directly coimmunoprecipitate hnRNP H1, hnRNP F, and, to a lesser extent, hnRNP H3. Utilizing a panel of mutants constructed in our laboratory, we demonstrate a correlation between the ability of these mutant proteins to regulate exon IIIc inclusion and the ability of the proteins to complex with hnRNP H1. It is worth noting that the panel of mutants for both hnRNP H1 and Fox2 identified mutations that reduced the levels of protein coprecipitated yet did not affect the splicing activity. We suggest that this could be explained if the ability of these mutants to complex remained above a minimum threshold required to maintain activity.

In addition to the coimmunoprecipitation experiment, we show that the presence of Fox2 enhanced the ability of hnRNP H1 to compete with ASF/SF2 in cross-linking to exon IIIc RNA. These data strongly suggest that there is a functionally relevant interaction of Fox proteins with the hnRNP H/F family. This interaction may have broader implications for the functions of these proteins, as Fox and hnRNP H and hnRNP F proteins share several intriguing similarities. Both families have atypical RNA binding domains, and both have been reported to function as both splicing silencers and splicing activators (3, 19). Interestingly, recent studies, which examined activity as it relates to binding context, arrived at similar results. Both Fox and hnRNP H and F tend to function as splicing activators when binding downstream of a regulated exon and splicing silencers when binding upstream of or within the regulated exon (4, 15, 26). These findings hint at a broader significance to the protein complex containing hnRNP H and F and the Fox proteins. They also suggest that this complex, including any additional proteins within it, should be investigated further.

As the number of proteins known to regulate the alternative splicing of FGFR2 has increased, one question that arises is how a small number of tissue-specific splicing factors could have such a dramatic impact on an exon that is already under the control of many ubiquitous proteins. As a result of the findings with hnRNP H and F and Fox, we propose a collapsible-network model. At the heart of this model is the observation that through protein-protein interactions, splicing factors can influence the affinity of another RNA binding protein to a nearby site on the RNA. This property has been proposed for splicing repressors such as hnRNP A and B proteins as well as enhancing SR proteins such as ASF/SF2 (40). It has also been proposed by our laboratory and others to occur during splicing silencing by PTB (33). In fact, the process of exon definition itself seems to depend on a network of protein interactions that allow communication between the 5′ splice site and the 3′ splice site and the subsequent formation of a commitment complex, and these RNA-protein interactions can be remodeled, as the phosphorylation of ASF/SF2 is able to alter the binding with splicing factor U1-70K (38).

The collapsible-network model posits that the network of SR proteins that bind to alternatively spliced exons depends upon these reinforcing protein-protein interactions to be sustained. The binding of one SR protein molecule can promote the recruitment of another molecule at a nearby site. This creates the potential for a positive-feedback loop; the binding of an SR protein at any given site is reinforced by the binding of other SR proteins to nearby sites, and, conversely, a potential for collapse, the displacement of an SR protein at a given site would subsequently decrease the binding affinity of SR proteins at other sites on the exon. In the case of FGFR2 exon IIIc, the binding of ASF/SF2 to the ESE that we identified is likely to depend upon the binding of additional SR proteins to nearby sites on the exon. This network of protein-protein interactions stabilizes the binding of each individual protein to the RNA, allowing the network to outcompete the ubiquitously expressed silencing factors that are present, such as the hnRNP H and hnRNP F proteins.

In epithelial cells, the presence of Fox proteins triggers a cascade that collapses the network of SR proteins, silencing the exon. In fact, Fox may nucleate the binding of a network of silencing factors as the binding of Fox to the RNA assists the binding of hnRNP H and hnRNP F to an ESS through stabilizing protein-protein interactions. Together, these proteins displace ASF/SF2 and other SR proteins from the RNA, thus triggering a chain reaction as the displacement of SR proteins from the RNA, resulting in exonic silencing.

Additionally, the collapsible-network model offers a simple explanation for the context-dependent opposing activities seen with some splicing factors such as Fox, hnRNP H, and hnRNP F. Instead of antagonizing a network of SR proteins, if the binding of these factors to the RNA were to displace a network of silencing factors, such as hnRNP A and hnRNP B or PTB, from the RNA, then the collapse of the silencing factors would allow the SR proteins to bind the RNA, activating splicing of the exon. In the case of FGFR2 exon IIIb, the binding of Fox proteins to the intron downstream of exon IIIb could theoretically disrupt the network of ubiquitous silencing factors, including PTB and hnRNP A1, that silence that exon. Thus, the binding of Fox and other unknown factors could displace the silencers from critical sites within the intron, triggering the collapse of the silencing network. Although this model is still speculative and the molecular mechanism is no doubt more

complicated, we feel that the collapsible-network model provides a mechanism to explain how cell-type-specific splicing factors could utilize or antagonize the numerous ubiquitously present splicing factors in order to remodel the protein complexes binding to the RNA and dramatically affect splicing. In order to test this model and better understand the mechanism of alternative splicing regulation, the protein-protein interaction of splicing factors needs to be characterized. This paper begins this process by establishing the hnRNP H and hnRNP F proteins as being silencers of FGFR2 exon IIIc and describing an interaction with Fox2 that allows the protein to antagonize the SR protein ASF/SF2.

ACKNOWLEDGMENTS

We thank Doug Black for generously sharing plasmids and an antibody for hnRNP H. We also thank Sebastian Oltean, Barbara Natalizio, and Jenny Mauger for reviewing the manuscript.

This research was supported by a PHS grant (R01 GM063090) to M.A.G.-B.

REFERENCES

1. **Abdul-Manan, N., S. M. O'Malley, and K. R. Williams.** 1996. Origins of binding specificity of the A1 heterogeneous nuclear ribonucleoprotein. Biochemistry **35:**3545–3554.
2. **An, P., and P. J. Grabowski.** 2007. Exon silencing by UAGG motifs in response to neuronal excitation. PLoS Biol. **5:**e36.
3. **Auweter, S. D., R. Fasan, L. Reymond, J. G. Underwood, D. L. Black, S. Pitsch, and F. H. Allain.** 2006. Molecular basis of RNA recognition by the human alternative splicing factor Fox-1. EMBO J. **25:**163–173.
4. **Baraniak, A. P., J. R. Chen, and M. A. Garcia-Blanco.** 2006. Fox-2 mediates epithelial cell-specific fibroblast growth factor receptor 2 exon choice. Mol. Cell. Biol. **26:**1209–1222.
5. **Black, D. L.** 2003. Mechanisms of alternative pre-messenger RNA splicing. Annu. Rev. Biochem. **72:**291–336.
6. **Caputi, M., and A. M. Zahler.** 2001. Determination of the RNA binding specificity of the heterogeneous nuclear ribonucleoprotein (hnRNP) H/H′/F/2H9 family. J. Biol. Chem. **276:**43850–43859.
7. **Caputi, M., and A. M. Zahler.** 2002. SR proteins and hnRNP H regulate the splicing of the HIV-1 tev-specific exon 6D. EMBO J. **21:**845–855.
8. **Carstens, R. P., J. V. Eaton, H. R. Krigman, P. J. Walther, and M. A. Garcia-Blanco.** 1997. Alternative splicing of fibroblast growth factor receptor 2 (FGF-R2) in human prostate cancer. Oncogene **15:**3059–3065.
9. **Carstens, R. P., W. L. McKeehan, and M. A. Garcia-Blanco.** 1998. An intronic sequence element mediates both activation and repression of rat fibroblast growth factor receptor 2 pre-mRNA splicing. Mol. Cell. Biol. **18:**2205–2217.
10. **Carstens, R. P., E. J. Wagner, and M. A. Garcia-Blanco.** 2000. An intronic splicing silencer causes skipping of the IIIb exon of fibroblast growth factor receptor 2 through involvement of polypyrimidine tract binding protein. Mol. Cell. Biol. **20:**7388–7400.
11. **Cartegni, L., and A. R. Krainer.** 2002. Disruption of an SF2/ASF-dependent exonic splicing enhancer in SMN2 causes spinal muscular atrophy in the absence of SMN1. Nat. Genet. **30:**377–384.
12. **Cartegni, L., J. Wang, Z. Zhu, M. Q. Zhang, and A. R. Krainer.** 2003. ESEfinder: a Web resource to identify exonic splicing enhancers. Nucleic Acids Res. **31:**3568–3571.
13. **Champion-Arnaud, P., C. Ronsin, E. Gilbert, M. C. Gesnel, E. Houssaint, and R. Breathnach.** 1991. Multiple mRNAs code for proteins related to the BEK fibroblast growth factor receptor. Oncogene **6:**979–987.
14. **Chen, C. D., R. Kobayashi, and D. M. Helfman.** 1999. Binding of hnRNP H to an exonic splicing silencer is involved in the regulation of alternative splicing of the rat beta-tropomyosin gene. Genes Dev. **13:**593–606.
15. **Chou, M. Y., N. Rooke, C. W. Turck, and D. L. Black.** 1999. hnRNP H is a component of a splicing enhancer complex that activates a c-*src* alternative exon in neuronal cells. Mol. Cell. Biol. **19:**69–77.
16. **Crawford, J. B., and J. G. Patton.** 2006. Activation of alpha-tropomyosin exon 2 is regulated by the SR protein 9G8 and heterogeneous nuclear ribonucleoproteins H and F. Mol. Cell. Biol. **26:**8791–8802.
17. **Del Gatto-Konczak, F., M. Olive, M. C. Gesnel, and R. Breathnach.** 1999. hnRNP A1 recruited to an exon in vivo can function as an exon splicing silencer. Mol. Cell. Biol. **19:**251–260.
18. **Dignam, J. D., R. M. Lebovitz, and R. G. Roeder.** 1983. Accurate transcription initiation by RNA polymerase II in a soluble extract from isolated mammalian nuclei. Nucleic Acids Res. **11:**1475–1489.
19. **Dominguez, C., and F. H. Allain.** 2006. NMR structure of the three quasi RNA recognition motifs (qRRMs) of human hnRNP F and interaction studies with Bcl-x G-tract RNA: a novel mode of RNA recognition. Nucleic Acids Res. **34:**3634–3645.
20. **Domsic, J. K., Y. Wang, A. Mayeda, A. R. Krainer, and C. M. Stoltzfus.** 2003. Human immunodeficiency virus type 1 hnRNP A/B-dependent exonic splicing silencer ESSV antagonizes binding of U2AF65 to viral polypyrimidine tracts. Mol. Cell. Biol. **23:**8762–8772.
21. **Expert-Bezancon, A., A. Sureau, P. Durosay, R. Salesse, H. Groeneveld, J. P. Lecaer, and J. Marie.** 2004. hnRNP A1 and the SR proteins ASF/SF2 and SC35 have antagonistic functions in splicing of beta-tropomyosin exon 6B. J. Biol. Chem. **279:**38249–38259.
22. **Garneau, D., T. Revil, J. F. Fisette, and B. Chabot.** 2005. Heterogeneous nuclear ribonucleoprotein F/H proteins modulate the alternative splicing of the apoptotic mediator Bcl-x. J. Biol. Chem. **280:**22641–22650.
23. **Han, K., G. Yeo, P. An, C. B. Burge, and P. J. Grabowski.** 2005. A combinatorial code for splicing silencing: UAGG and GGGG motifs. PLoS Biol. **3:**e158.
24. **Jacquenet, S., A. Mereau, P. S. Bilodeau, L. Damier, C. M. Stoltzfus, and C. Branlant.** 2001. A second exon splicing silencer within human immunodeficiency virus type 1 tat exon 2 represses splicing of Tat mRNA and binds protein hnRNP H. J. Biol. Chem. **276:**40464–40475.
25. **Liu, H. X., L. Cartegni, M. Q. Zhang, and A. R. Krainer.** 2001. A mechanism for exon skipping caused by nonsense or missense mutations in BRCA1 and other genes. Nat. Genet. **27:**55–58.
26. **Martinez-Contreras, R., J. F. Fisette, F. U. Nasim, R. Madden, M. Cordeau, and B. Chabot.** 2006. Intronic binding sites for hnRNP A/B and hnRNP F/H proteins stimulate pre-mRNA splicing. PLoS Biol. **4:**e21.
27. **Mayeda, A., S. H. Munroe, J. F. Caceres, and A. R. Krainer.** 1994. Function of conserved domains of hnRNP A1 and other hnRNP A/B proteins. EMBO J. **13:**5483–5495.
28. **Mayeda, A., S. H. Munroe, R. M. Xu, and A. R. Krainer.** 1998. Distinct functions of the closely related tandem RNA-recognition motifs of hnRNP A1. RNA **4:**1111–1123.
29. **Min, H., R. C. Chan, and D. L. Black.** 1995. The generally expressed hnRNP F is involved in a neural-specific pre-mRNA splicing event. Genes Dev. **9:**2659–2671.
30. **Rooke, N., V. Markovtsov, E. Cagavi, and D. L. Black.** 2003. Roles for SR proteins and hnRNP A1 in the regulation of c-*src* exon N1. Mol. Cell. Biol. **23:**1874–1884.
31. **Smith, P. J., E. L. Spurrell, J. Coakley, C. J. Hinds, R. J. Ross, A. R. Krainer, and S. L. Chew.** 2002. An exonic splicing enhancer in human IGF-I pre-mRNA mediates recognition of alternative exon 5 by the serine-arginine protein splicing factor-2/alternative splicing factor. Endocrinology **143:**146–154.
32. **Smith, P. J., C. Zhang, J. Wang, S. L. Chew, M. Q. Zhang, and A. R. Krainer.** 2006. An increased specificity score matrix for the prediction of SF2/ASF-specific exonic splicing enhancers. Hum. Mol. Genet. **15:**2490–2508.
33. **Wagner, E. J., and M. A. Garcia-Blanco.** 2001. Polypyrimidine tract binding protein antagonizes exon definition. Mol. Cell. Biol. **21:**3281–3288.
34. **Wang, E., N. Dimova, and F. Cambi.** 2007. PLP/DM20 ratio is regulated by hnRNPH and F and a novel G-rich enhancer in oligodendrocytes. Nucleic Acids Res. **35:**4164–4178.
35. **Wang, J., P. J. Smith, A. R. Krainer, and M. Q. Zhang.** 2005. Distribution of SR protein exonic splicing enhancer motifs in human protein-coding genes. Nucleic Acids Res. **33:**5053–5062.
36. **Wang, Z., M. E. Rolish, G. Yeo, V. Tung, M. Mawson, and C. B. Burge.** 2004. Systematic identification and analysis of exonic splicing silencers. Cell **119:**831–845.
37. **Woppmann, A., C. L. Will, U. Kornstadt, P. Zuo, J. L. Manley, and R. Luhrmann.** 1993. Identification of an snRNP-associated kinase activity that phosphorylates arginine/serine rich domains typical of splicing factors. Nucleic Acids Res. **21:**2815–2822.
38. **Xiao, S. H., and J. L. Manley.** 1997. Phosphorylation of the ASF/SF2 RS domain affects both protein-protein and protein-RNA interactions and is necessary for splicing. Genes Dev. **11:**334–344.
39. **Zahler, A. M., C. K. Damgaard, J. Kjems, and M. Caputi.** 2004. SC35 and heterogeneous nuclear ribonucleoprotein A/B proteins bind to a juxtaposed exonic splicing enhancer/exonic splicing silencer element to regulate HIV-1 tat exon 2 splicing. J. Biol. Chem. **279:**10077–10084.
40. **Zhu, J., A. Mayeda, and A. R. Krainer.** 2001. Exon identity established through differential antagonism between exonic splicing silencer-bound hnRNP A1 and enhancer-bound SR proteins. Mol. Cell **8:**1351–1361.